Structural and Multidisciplinary Optimization (2025) 68:29
https://doi.org/10.1007/s00158-024-03914-8

RESEARCH PAPER

Constructability-based multi-objective optimization with machine learning-enhanced meta-heuristics for reinforcing bar design in rectangular concrete columns

Luis F. Verduzco[1]

Received: 25 June 2024 / Revised: 3 September 2024 / Accepted: 22 October 2024

Abstract
Optimization of reinforcing bar (rebar) design represents a preponderant factor in reducing material usage and wastes for reinforced concrete (RC) structures. The assessment of constructability of such rebar designs is crucial to improve their practicality and reduce construction costs, which makes the problem multi-objective (MO). However, when applying optimization methods for the design of rebar in RC structures, little attention has been paid on columns, in comparison to beams and slabs. Meta-heuristic algorithms (MA) have been the ones mostly deployed for these types of elements, which have proven to be of high computational cost. Additionally, an existing gap in the literature as to how to relate the design and construction stage of rebar in RC structures through constructability analysis is evident. In this regard, research has been focused mainly at the building level but not at the element level. This works presents a novel algorithmic framework using Machine Learning (ML)-enhanced meta-heuristics for the optimal design of rebar on rectangular RC columns. To assess the constructability of the resulting rebar layouts a Buildability Score (BS) model at the element level is proposed. The complexity analysis of rebar design under the constructability restrictions, through combinatorial optimization (CO), is used to assess the global time efficiency of the framework. The Non-Sorting Genetic Algorithm II (NSGA-II) was deployed for showcase and five different ML algorithms were used to enhance it, namely the *k*-NN classifier, SVM regression, ANN, Gauss Process (GP) regression, and Tree Ensembles (TE), where the latter three showed the best performance.

Keywords Reinforced concrete · Buildability score model · Machine learning-enhanced meta-heuristics · Rebar design · Multi-objective optimization · Rectangular columns

1 Introduction

Global warming is nowadays more critical than ever and the construction industry plays an important role in it with approximately 33% of the total CO_2 emissions (Chai et al. 2022). Thus, architects, structural engineers, and constructors are increasingly faced with new challenges to create more environmentally friendly building designs. In this regard, reinforced concrete (RC) is usually the preferred material in comparison to steel, mostly for tall buildings but also for many other types of civil infrastructure (Devenes et al. 2024). Approximately between 15 and 20 billion m^3 of RC are produced annually in the world (Tanhadoust et al. 2023) with only a limited portion of it being reused (Devenes et al. 2024).

Under this context, new needs have been set in the area of RC design for the reduction of demolition waste and enhancement of construction productivity. This had led, in turn, to the emergence of new paradigms in the Architecture, Engineering and Construction (AEC) industry related to digital fabrication techniques, such as the Design of Manufacturing of Assembly (DfMA; Afzal et al. 2017). This paradigm promotes the development of new methodologies, frameworks and automation techniques for optimal Performance-Based Designs (PBD) of RC structures. In this regard, researchers highly suggest to pay special attention to the optimization of steel reinforcement (Afzal et al. 2020). One of the reasons is that reinforcing steel has proven to have

Responsible editor: Mehmet Polat Saka

Luis F. Verduzco
lfvm@connect.ust.hk

[1] Department of Civil & Environmental Engineering, The Hong Kong University of Science and Technology (HKUST), Clear Water Bay, New Territories, Hong Kong

Published online: 15 February 2025

the highest share in the embodied energy of RC buildings of over 66% in comparison to the concrete of approximately 60% (Moussavi Nadoushania and Akbarnezhad 2015).

Moreover, due to the remarkable development of computational tools to conceptualize buildings, such as Building Information Modeling (BIM), nowadays architects are more inclined to propose very irregular geometries because of their esthetic nature (Afzal et al. 2020). However, such irregularities complicate the design process to ensure a proper mechanical behavior. Given that their geometry is irregular its stiffness is also irregular, with respect to any axis of reference. Such irregularity in stiffness promotes the development of asymmetrical bending loads on columns under any action considered (Fig. 1). To address this issue, the reinforcement in columns must be designed to guarantee an efficient resistance and ductility level, while at the same time using the least possible material. An optimization problem, thus, arises, which requires to take the design of such reinforcement to another optimal level, most likely with asymmetrical rebar configurations (Lee et al. 2009; Gil-Martín et al. 2010).

It has been demonstrated in the literature that savings of approximately 50% of rebar volumes could be generated with optimal asymmetrical rebar (Gil-Martín et al. 2010; Aschheim et al. 2018; Carbonell-Márquez et al. 2014). However, despite of these facts, asymmetrical optimal reinforcement remains an open study. The issue is that many uncertainties arise when dealing with these designs for columns. For structural engineers and designers, the concern tends to be in regard to the reduction of axial resistance that short columns with asymmetrical rebar present (L'udovit et al. 2013). However, such disadvantage could be balanced by adding heavy confinement. Hernández-Montes et al. (2004), for instance, demonstrated that asymmetrical longitudinal rebar designs in heavily confined rectangular cross-sections enhanced the curvature ductility capacity. For constructors, the problem with asymmetrical rebar designs in columns is more related to the increase of unit construction costs in comparison to symmetrical ones. Given that asymmetrical rebar configurations are more complex, it would take more time for workers to assemble it properly in-site, than conventional symmetrical designs. Thus, their *constructibility* is compromised, which makes the optimization problem of rebar, multi-objective in nature, due to its trade-off relationship with construction costs.

In this regard, constructability has become in recent years a crucial metric when moving toward industrialized construction (Li et al. 2021; Fischer and Tatum 1997), as it enables to link more effectively the design process of structures with their construction. Even though these such labor tasks of rebar assembly will be more likely automated by robotics systems in future decades (García de Soto et al. 2018; Bock 2015), there is still a long way ahead until they are fully integrated into the standardized process of building design and construction. Until then, initial steps must be put forward to measure the constructability of rebar designs, not only for columns but for any RC structure, and optimize under this measure. Nevertheless, up to now, the research to measure constructability focuses mostly at the building level, not at the individual element level, and the lack of Buildability Score (BS) models specifically for rebar design is evident.

As for the solution of this multi-objective optimization problem, meta-heuristics represent a very reliable approach (Afshari et al. 2019). However, it has been demonstrated that such algorithms alone require usually a high computational cost demand (Afzal et al. 2020; Afshari et al. 2019; Sánchez-Olivares and Tamas 2017). To reduce such demand ML techniques could be used to enhance meta-heuristics. This algorithmic framework, however, remains up to this day unexploited for optimization design

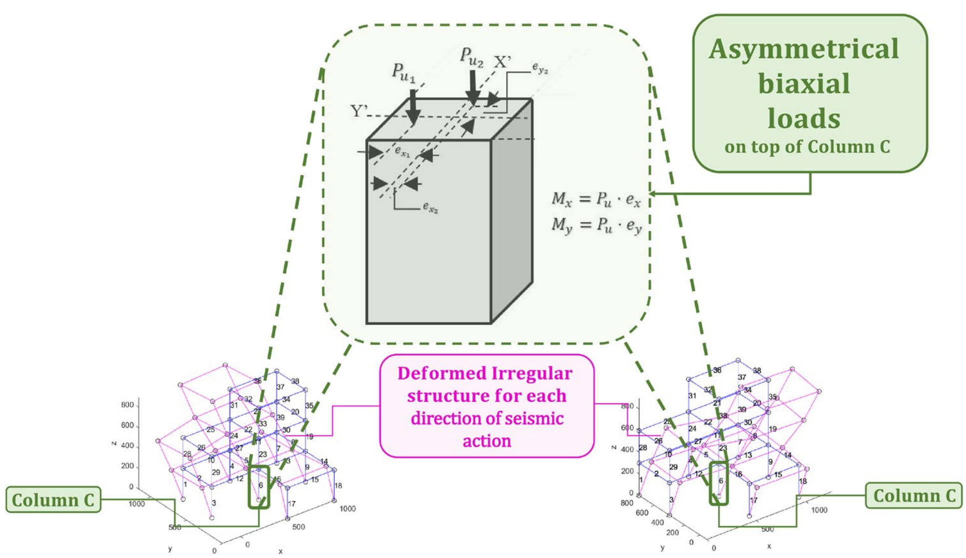

Fig. 1 Depiction of an irregular 3D frame whose columns are subject to considerably asymmetrical biaxial bending loads due to seismic actions

of RC columns, in the literature. Even though some efforts can be found with Artificial Neural Networks (ANN) and Support Vector Machines (SVM), most of the research focuses on continuous beams, slabs (Li et al. 2021; Yuan et al. 2018), shear walls (Lou et al. 2021; Alanani et al. 2024), or free clash optimization in joints (Zhao et al. 2024), paying little attention to columns, for which usually only symmetrical rebar designs are considered.

This work presents the development of an algorithmic framework with Machine Learning Enhanced (ML-Enhanced) Meta-heuristics for the optimization design of rebar in rectangular concrete columns subject to either uniaxial or biaxial bending. To approach the problem, a novel BS model, specifically for rebar in concrete columns at the individual level, is proposed. Such model enables to measure the constructability of rebar designs and its relationship to their construction costs. Five different ML algorithms are tested, namely the *k*-NN classifier, SVM regression, ANN, Gaussian Process (GP) regression, and Tree Ensembles (TE). Both Single Objective (SO) and Multi-Objective (MO) optimization algorithms are used to assess the efficiency of each ML technique to enhance meta-heuristics. For SO, the Particle Swarm Optimization (PSO) and Genetic Algorithm (GA) are considered. Whereas for MO, the Non-Sorting Genetic Algorithm II (NSGA-II) is deployed. To assess the efficiency for SO optimization, a complexity analysis of rebar design has been developed based on combinatorial optimization (CO). This complexity analysis enables to determine the sample solution space of rebar designs as the cross-section dimensions of the columns change, through an average worst case complexity. Such average worst case scenario is considered as base of comparison to assess the time and convergence efficiency of the SO optimization processes here developed. As for the MO optimization algorithms, the Mean-Inverted Generational Distance (MIGD) is used to assess the convergence efficiency of each ML-Enhanced NSGA-II. Such comparison is made in relation to an optimal Pareto Front (PF) of reference, determined through a Non-Enhanced two-stage NSGA-II.

This work aims at finally closing the gap between meta-heuristic optimization and ML for the optimal design of reinforcement in concrete columns, in reasonable computational execution times. It is expected that with this research the state-of-the-art of asymmetrical optimal rebar for concrete columns may be broaden and therefore, its popularity in industrial practice, so that in the long term, commercial software of structural analysis and design can be capable to determine such optimal designs as part of their main functions. This approach of optimization represents a key factor for more sustainable building and design practices of RC structures, to mitigate environmental impacts caused by material usage and wastes.

2 Literature review

2.1 Optimization methods for the design of rebar in RC structures

Regarding the development of computational methods for the optimal design of rebar for RC structures, meta-heuristic algorithms rapidly became of the most deployed ones (Afzal et al. 2020), especially the GA (see for examples Lepš and Sejnoha 2003; Rafiq and Southcombe 1998; Coello et al. 1997; Koumousis and Arsenis 1998 corresponding to works focused on columns and beams). Up to this day, however, with the new available technologies in computational software and programming interfaces, more refined analysis and optimal design procedures are possible. In Afzal et al. (2020), a state-of-the-art review was made to identify the types of RC structures most explored with optimization methods. It was found that most of the research has been focused on RC frames (see for instance Liu et al. 2020; Mangal et al. 2021; Xu et al. 2022 related to optimization design frameworks of RC frames with BIM software). Whereas related research for columns was, surprisingly, found to be of the least, despite their major importance for structural systems and the potential that optimization rebar techniques have for such elements. In Afzal et al. (2020) the most deployed optimization algorithms for the design of RC structures were also identified. It was found that mostly pure meta-heuristics have been developed (see for examples of relevant works Jahjouh et al. 2013; Gandomi et al. 2015; Barros et al. 2004; Raue and Hahn 2005; Pierott et al. 2021, corresponding to optimal designs for concrete columns, beams, and retaining walls). However, when it comes to the development and application of pure ML models up until 2020 only ANN have been used and with a limited number of studies. Some relevant works are Fernández-Ceniceros et al. (2013), Ahmadkhanlou and Adeli (2005), and Yeh and Chen (2012) in which ANN were used, although only focused on slabs and beams. More recent similar works after 2020 include Zhao et al. (2024) where Graph Neural Networks (GNN) were used, although only for shear wall structures.

The reason why meta-heuristics and stochastic optimization methods became so widely popular is due to their versatility in adapting to problems of multiple variables. These types of problems is exactly what a structural designer faces when designing a RC section, especially for those subject to biaxial load combinations, such as columns (Sánchez-Olivares and Tamas 2017). Also, their higher likeliness to reach optimal global solutions in comparison with classical optimization methods makes them preferable (Wahde 2008). However, until now, practically all the algorithms developed with meta-heuristics for any RC element have demonstrated to require a great computational demand (Afzal et al. 2020). The issue lies mainly on the great number of potential feasible solutions of rebar designs that can be found for a given concrete column section. It is of such complexity that several researchers have actually referred to it to be an NP-hard problem (Afzal et al. 2020). Even though some efforts have been made to decrease the computational effort of such algorithms (as in Sánchez-Olivares and Tamas 2017 with the exploration of tuning parameters for different algorithms) there is still a lot to achieve when aiming toward their deployment for complex structural systems of numerous elements/columns.

2.1.1 ML-Enhanced meta-heuristics for optimization design of RC structures

A key factor to reduce the computational power demand for optimization design of RC structures is the introduction of ML models as aiding techniques for optimization design algorithms. When referring to this optimization framework for structural engineering, in general, it is important to distinguish between ML-based optimization for estimation and ML-based optimization for design. When it comes, specifically, to the deployment of this framework for RC structures, most of the research in the literature is usually focused on optimized prediction and estimation. The existing research is diverse, both in the type of prediction and types of structures in question. The applications range from structural failure classification with ANN and the NSGA-II (Chatterjee et al. 2007), bond strength and failure mode prediction with TE and GA (Mahmoudian et al. 2023), shear capacity prediction for RC shear walls (Chou et al. 2022), and even for predictions of fundamental periods of vibration of RC frames (Latif et al. 2022).

However, when referring to ML-based optimization for design, the state-of-the-art research is considerably less than for prediction, especially for RC columns. Under this context, only counted research works have been found in the literature in which some sort of previous knowledge was used to aid their optimization design procedures for columns. In Aschheim et al. (2007), for instance, optimal constrained domains for uniaxial bending were built. In Gil-Martín et al. (2011), the development of a theorem was made to approximate the optimal solution for a specific set of load combinations based on the construction of small databases. For the latter, however, many assumptions and simplifications were made making the theorem also only applicable for uniaxial bending actions. It has not been until this 2020s decade that the well-defined ML techniques have been used to aid meta-heuristics for optimal design of RC structures, although mainly focused on beam elements, floors, shear walls and free clash in column beam joints of RC frames. In Li et al. (2023), for instance, GNN were used to enhance an Exploratory Genetic Algorithm (EGA), demonstrating great advantages in relation to pure meta-heuristics, both in time and convergence efficiency. This approach, however, was mainly focused on free clash rebar design optimization. Other related works of ML-based optimization of RC structures include Lou et al. (2021), where the Tabu Search algorithm was enhanced with SVM for the optimization design of shear walls in tall buildings, or Alanani et al. (2024) where ANN were used to enhance the NSGA-II for the optimization design of RC tall buildings, although considering only conventional symmetrical reinforcement on the column elements.

Aydın et al. (2023) and Nigdeli et al. (2023) have made some efforts in the last couple of years, for optimization design of columns with ML-enhanced meta-heuristics. They used the Harmony Search HS algorithm as the main optimization procedure and several ML models were tested as enhancement. It was found that Tree-Ensemble models had the best performance, with quite high levels of accuracy. Their research, however, has only been focused on Single Objective optimization of columns under uniaxial bending and therefore, have not paid proper attention to the optimal distribution of rebars in an asymmetrical fashion from a biaxial perspective. Moreover, their research is not fully focused on the optimization of the rebar itself, as it considers also the columns' cross-section dimensions as optimization variables. Additionally, it does not present a proper analysis of time efficiency of the algorithms developed, neither in relation to the whole search space considered nor in relation to the required computational time for the meta-heuristics alone without ML enhancement. The last part of analysis, concerning time efficiency, is crucial for the promotion of this optimization design approach in commercial industrial software.

2.2 Constructability analysis for rebar designs

Regarding that few research focused on RC column elements, however, the *constructability* of the resulting layouts of rebar has not been yet fully addressed. Most of the research in this area applies for structural systems and buildings, focusing mainly on improving installation (Chen et al. 2010), resource availability (Pasandideh et al. 2015), logistics (Chen et al. 2017), or standardization (Lao et al. 2023). Among the few research works that have been found to have somehow addressed a constructability metric of rebar designs for individual structural RC elements, either focus on other types of elements, such as floors (Eleftheriadis et al. 2018) and beams (Mangal and Cheng 2018) with little attention to columns. In Mangal and Cheng (2018), for instance, the optimal designs for columns based on some sort of constructability metric only considered the asymmetry of rebar with respect to one reference axis, specifically the relationship between *the amount of reinforcement in compression and that in tension*. This uniaxial condition, however, would only exist for 2D RC frames without considering rebars in between those two edges. Due to the efficiency of confining reinforcement, such uniaxial asymmetrical rebar designs in columns do not represent a practical solution. In Lao et al. (2023), a constructability metric for the design of rebar in columns was also developed, although only symmetrical rebar designs were considered.

Additionally, to effectively assess the constructability of a rebar design in an RC structural element the development of Buildability Score BS models becomes essential. It has been suggested in the literature that such BS models enable the integration between design and practice stages of infrastructure projects in the AEC industry (Adams 1989). Thus, through the development of these sort of models, specifically for rebar in concrete structures at the element level, more proper estimations of construction costs would be enabled, as well as the relationship with their practicality or with any other variable of interest. Such control of variables has great potential for CO_2 emission optimization processes (Park et al. 2014; Yeo and Gabbai 2011), for which the relationship between environmental impact and construction cost is of great relevance to promote optimization design. Lastly, by focusing on measuring constructability of rebar designs at the element level, through BS models, further ones could be developed at the building level, based on them. This would enhance the quality and practicality of reinforcement design in RC structures, in general, as well as their sustainability.

3 Optimization design of rebar in rectangular concrete columns

Symmetrical conventional designs in columns do not represent a sustainable option anymore, just by means of environmental impact. They are only fit when symmetrical load combinations on columns are generated (Fig. 2, Left), with respect of each cross-section's axis. In general, the higher the asymmetry between the load combinations, the most likely an asymmetrical rebar design would be the optimum solution (Sánchez-Olivares and Tamas 2017). In fact, asymmetrical biaxial loads on columns and similar types of structures are of the most common ones to be developed. Clear examples include columns in irregular buildings or piers in irregular bridges. Other examples include retaining walls and earth retaining piers, among others.

When asymmetrical biaxial loads are present and asymmetrical rebar designs are the most fit option it is crucial to pay special attention to their practicality. Given their asymmetrical distribution of number of rebars and/or diameters in the column, it would take more time for workers in-site to assemble them correctly than symmetrical conventional designs. In this sense, even though important savings of material could be generated with asymmetrical rebar designs, their constructability would be compromised, which would affect, in turn, their construction cost. Thus, when designing asymmetrical optimal rebar in columns it is preponderant to consider certain restrictions of distribution. It is through such set of restrictions and the way in which the irregularity of the distributions of rebars are penalized, what would constitute a Buildability Score model, to measure their constructability.

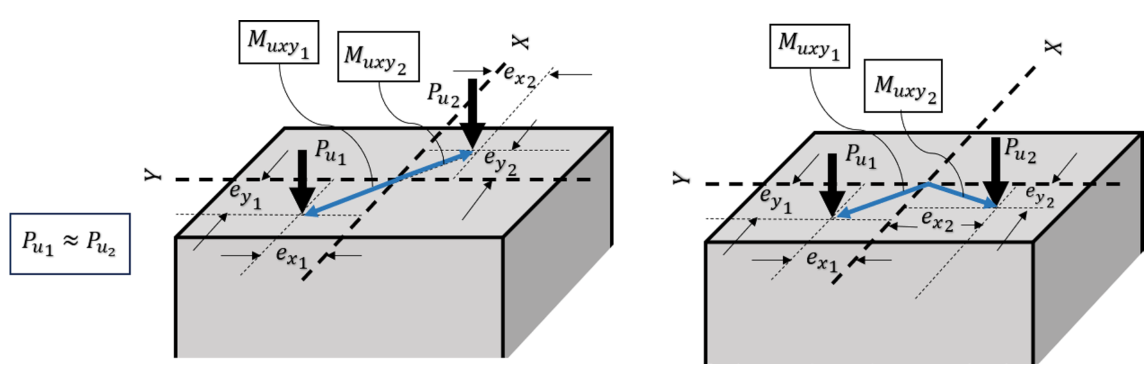

Fig. 2 Biaxial loads on a rectangular concrete column with respect to each cross-section's axis. Left: symmetrical loads. Right: asymmetrical loads

3.1 Constructability of rebar design in rectangular concrete columns

By definition, constructability is *the optimum use of construction knowledge and experience in the conceptual planning, engineering, procurement and field operations phases to achieve the overall project objectives* (Adams 1989). One major problem in construction sites is the lack of integration of this practice through the interaction between the design and the construction stage. In Asia, Singapore has pioneered with the quantification of constructability for buildings based on a scheme known as the Buildable Design Appraisal System (BDAS), which culminated in a minimum requirement for building designs to comply with, known as the *Buildability Score (BS)*. This BS model takes into account the level of standardization, simplicity, and extent of integrated elements used in the design of a building (BCA 2004) to measure its easiness of construction. Even though it is specifically adapted on the building level, the same concepts and principles could be adopted to develop BS models on the structural element level. Here we attempt to extend such principles for constructability assessment of rebar designs in rectangular concrete columns.

In this context, it would be beneficial for constructability purposes to take advantage of the column's geometry itself. In similar works found in the literature for rectangular concrete columns, researchers have proposed implicitly and explicitly certain distribution constraints (Hernández-Montes et al. 2004; Gil-Martín et al. 2010; Aschheim et al. 2018; Lee et al. 2009; Sánchez-Olivares and Tamas 2017). Perhaps, the most common one adopted consists of limiting the number of rebar diameters over the cross-section to a max of four, with only one diameter size per cross-section's boundary, as presented in Fig. 3. In this sense, the number of rebars to be placed at each of such boundaries would only be limited by the constraint of min rebar separation sep_{min} that may be considered from the applicable design code.

Hence, to measure the constructability of rebar designs in rectangular concrete columns, the previous set of restrictions of rebar distribution over the column's cross-section can be considered. This way, a certain level of practicality with respect to conventional symmetrical designs, of the resulting most likely asymmetrical ones, would be ensured. In this regard, the following variables for the BS model are proposed:

Uniformity of Number of rebars. For RC rectangular columns, the *Uniformity of Number of Rebars* (UNB) over the cross-section is a preponderant factor to estimate the buildability of a design, so that the asymmetry of the distribution of number of rebars at each cross-section's edge with respect of each cross-section's axis can be measured, as shown in Fig. 4. In such figure the variables nb_1, nb_2, nb_3, nb_4 are defined as the number of rebars at top, bottom, left, and right edges of the cross-section, respectively.

By code provisions, the total number of rebars in a rectangular column cross-section is at minimum four. Such restriction is expressed by $nb_1, nb_2 \geq 2$, so that $nb_3, nb_4 \geq 0$. A good estimator of this such uniformity factor of distribution of number of rebars could be formulated as follows (1):

$$\mathrm{UNB} = \frac{1}{2}\left(\frac{\min(nb_1, nb_2)}{\max(nb_1, nb_2)} + \frac{\min(nb_3, nb_4)}{\max(nb_3, nb_4)}\right). \tag{1}$$

As one can derive, $\mathrm{UNB} \in [0, 1]$. In the extreme case of full symmetry ($nb_1 = nb_2$ and $nb_3 = nb_4$), $\mathrm{UNB} = 1$, vice versa, when $nb_1 \ll nb_2$ and $nb_3 \ll nb_4$, $\mathrm{UNB} \rightarrow 0$.

Uniformity of sizes of Rebar Diameters. Another important factor to consider is the total Number of distinct rebar Diameters over a single cross-section (ND), which is recommended to be a maximum of four, i.e., $\mathrm{ND} \in [1, 4]$, as shown in Fig. 3. Generally, fewer rebar diameters are more favorable to enhance the construction productivity, given that these rebar sizes are sold by tons. However, in certain cases, the diversity of rebar diameters could be preferred, for example, when it is required to reuse existing rebar cut wastes. Such preference could be expressed

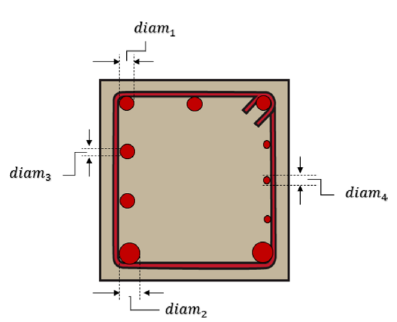

Fig. 3 Basic restriction of rebar distribution in rectangular concrete columns: a max of four sizes of rebar diameters can be placed. Only one size of diameter can be placed at each cross-section's boundary

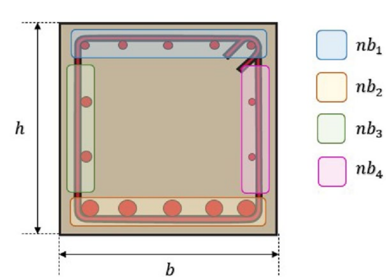

Fig. 4 Description of the variables involved for the estimation of the parameter *Uniformity of Number of Rebars UNB* to measure the asymmetry of the distribution of number of rebars over a rectangular column cross-section

as weight factors when formulating the estimation model of the Buildability Score for rebar designs in columns, so that they can be adjusted for each particular design case.

Constructability Score. Thus, our final BS model combines the two desired as follows:

$$BS = UNB^{W_{UNB}} + \frac{1}{ND^{W_{ND}}}, \tag{2}$$

where W_{UNB} is the weight factor of the variable UNB and W_{ND} is the weight factor of the variable ND. It is through such weight factors that the preference between variability in number of rebars against variability of rebar diameters can be expressed in the BS model, according to the needs of each special construction project. A closer look at this such model shows that it can only take values between the following range [0, 2].

The more symmetrical and uniform the rebar design the higher the BS. As it could be inferred, the BS of each rebar designs affects only the assembly performance of that design executed by workers in site. In this sense, a rebar design with a BS value of 1 would indicate that it would take twice as much the time of assembling for a symmetrical conventional design. One efficient way to integrate the BS into the estimation of construction costs of rebar designs is to normalize it so that the original assembly performance based on the most simple and symmetrical rebar design (with only one rebar diameter and symmetrically distributed number of rebars) is factorized by such normalized value, referred to as the *Constructability Factor of rebar Assembly CFA*. Thus, this factor could be estimated as $0 < [CFA = BS/2] \leq 1$. A numerical breakdown of this constructability model is presented, in detail, in "Appendix 7."

3.2 Optimization variables

When formulating an optimization design formulation for rebar design in columns, several optimization variables can be considered. In Sánchez-Olivares and Tamas (2017), for instance, the rebar diameters, the number of rebars at each cross-section's boundary, the depth of the neutral axis, and angle of the neutral fiber were considered as the main optimization variables. Such choice of design variables results in a high-dimensional search space, rendering it challenging to scale too many columns (Sánchez-Olivares and Tamas 2017). However, when designing a column, the neutral axis depth is usually just sought to be constrained to a specific max value to ensure a certain level of desired column ductility, and not as a design variable. For this such scenario, the neutral fiber angle can be considered to be just a feature of the neutral axis itself. In this sense, the number of design variables for optimization design of reinforcement in columns can be reduced to only eight, i.e., four for the number of rebars at each cross-section's edge nb_1, nb_2, nb_3, nb_4 and four for the rebar diameter sizes db_1, db_2, db_3, db_4. Nonetheless, the simplified problem itself is still NP complete and challenging to solve (Afzal et al. 2020) and as it is demonstrated in "Appendix 1" and "2."

Considering that our only focus is on rebar optimization, we set constant cross-section dimensions of the column b and h through the optimization design process. The compressive strength of the concrete f_c', the modulus of elasticity of the reinforcing steel E_s, and the yield stress of the reinforcing steel f_y are also set as constant.

3.2.1 Decomposed optimization problem with ML enhancement

As it could be easily derived, the max values for the discrete optimization variables nb_1, nb_2, nb_3, nb_4 (corresponding to the number of rebar diameters at each of the cross-section's

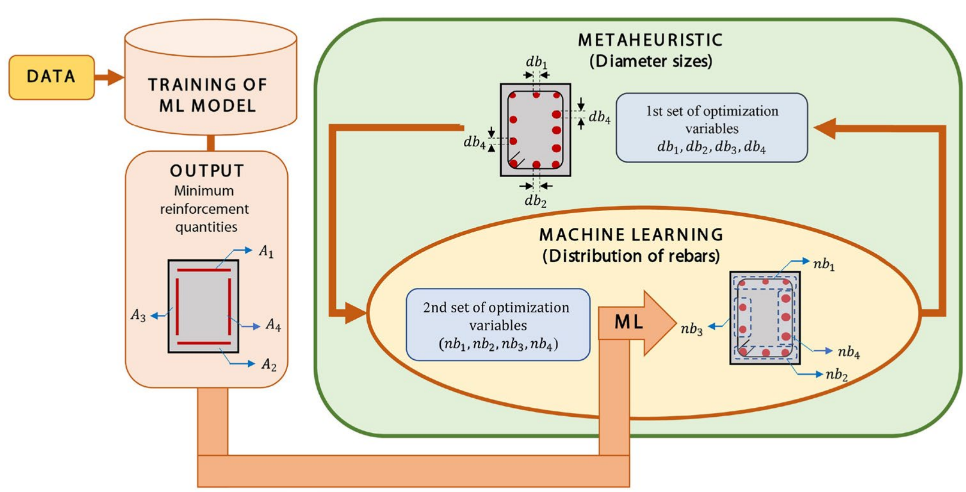

Fig. 5 Leveraging of metaheuristics with ML models for the optimal design of rebar in rectangular concrete columns through decomposed optimization

edges of a column) would be a function of the other set of discrete optimization variables $\mathrm{db}_1, \mathrm{db}_2, \mathrm{db}_3, \mathrm{db}_4$ (corresponding to the rebar diameters at each edge), the rebar separation code restrictions and the cross-section dimensions b,h of the column. As demonstrated in (17) from "Appendix 1", the complexity of the number of possible combinations of number of rebars for each combination of rebar diameters is $O(b^4)$. However, many of these possible design solutions would not even comply with the design restrictions imposed by code. Thus, for large cross-section dimensions, it would be beneficial, in regard to computational time, to decompose the optimization problem. This way, ML models could be built to aid a meta-heuristic optimization algorithm by taking care of the optimization set of variables concerning the number of rebars at each cross-section's edge, as shown in Fig. 5.

Under this approach and as it could be easily deduced, the number of possible combinations of sizes of rebar diameters over a rectangular cross-section, based on our proposed BS model, has complexity $O(\mathrm{ND}^4_{\mathrm{com}})$, where $\mathrm{ND}_{\mathrm{com}}$ is the number of available commercial rebars in the market, to choose from. Such number of available commercial rebar diameters is quite diverse nowadays, all around the world, and it ranges usually between 5 and 14 different sizes (McCormac and Brown 2013). Thus, by considering only the rebar diameters as optimization variables, the total number of possible design solutions that an optimization process would deal with, for the worst case scenario, will be $14^4 = 38,416$. This is just another reason why it is important to leverage meta-heuristics for the optimization of rebar design, so that they can focus entirely on the sizes of rebar diameters.

3.3 Design constraints

The ACI-318 code (ACI 2019) is considered to set the design constraints of rebar design. The following main constraints (3), (4), (5) apply, concerning to the max and min rebar cross-section area, the min rebar separation and the structural efficiency. For the latter, the computation of interaction surfaces was performed, as depicted in Fig. 6 for reference, where $M_{\mathrm{R}} = \phi M_{\mathrm{n}}$, with ϕ being the reduction resistance factor defined as follows (6):

$$[0.01bh \leq A_{\mathrm{s}} \leq 0.04bh], \quad , \tag{3}$$

$$\mathrm{sep}_{\min} = \max \begin{cases} \frac{4}{3}d_{\mathrm{ag}}, \; d_{\mathrm{ag}} = \frac{3}{4}in, \\ \frac{3}{2}d_{\mathrm{b}}, \end{cases} \quad , \tag{4}$$

$$\mathrm{Eff} = \frac{Q_{\mathrm{u}}}{Q_{\mathrm{R}}} = \frac{\sqrt{P_{\mathrm{u}}^2 + M_{\mathrm{u}}^2}}{\sqrt{P_{\mathrm{R}}^2 + M_{\mathrm{R}}^2}} < 1, \quad . \tag{5}$$

$$\phi = \begin{cases} 0.65 + (\epsilon_{\mathrm{t}} - 0.002)\frac{250}{3} & 0.004 \leq \epsilon_{\mathrm{t}} < 0.005, \\ 0.9 & \epsilon_{\mathrm{t}} > 0.005, \end{cases} \quad , \tag{6}$$

$$\epsilon_{\mathrm{t}} = \frac{0.003(d-c)}{c}. \quad . \tag{7}$$

Additional constraints include the max neutral axis depth c (8) and the max separation of rebars in the tension faces (9):

$$c \leq \frac{d}{\frac{0.005}{0.003} + 1}, \quad , \tag{8}$$

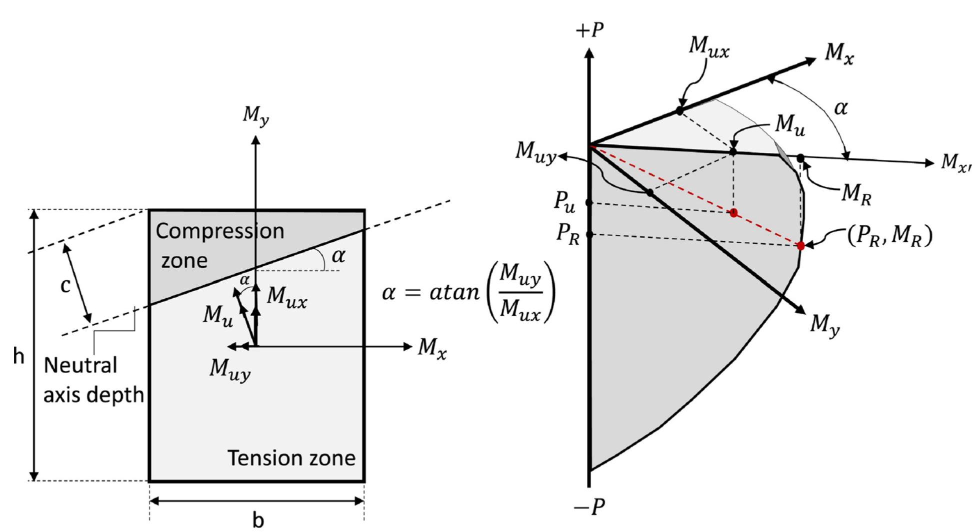

Fig. 6 Computation of the resistance efficiency for each column rebar design through 3D interaction surfaces

$$\mathrm{sep}_{\max} = \min \begin{cases} 380\left(\frac{280}{\frac{2}{3}f_y}\right) - \frac{5}{2}\mathrm{cover}, \\ 304\left(\frac{280}{\frac{2}{3}f_y}\right). \end{cases} \quad . \tag{9}$$

3.4 Formulation of the multi-objective optimization problem

Differing with what happens in a SO optimization problem in which a comparison of $f(x_1)$ with $f(x_2)$ is made directly to determine if a solution set x is better than another, in MO optimization the term *dominance* takes place to compare a variable set x of a function with another function. Thus, in a MO optimization problem not only one optimal solution of x can be obtained but a family of solutions through a *Pareto Front* mapping (Coello et al. 2007). For multi-objective optimization design of rebar in columns from a constructability point of view, the problem can be stated in terms of construction cost or rebar usage. When the problem is stated in terms of construction cost, it can be expressed mathematically as in Eq. (10), where x is the decision vector composed by the $n = 4$ variables just mentioned previously (namely the discrete variables corresponding the rebar diameters at each of the four cross-section's edges). S is the feasible objective space with $m = 2$ objective functions, namely the total construction cost C_s of reinforcement $f_1(x)$ and the constructability CFA f_2, under the $i = 1, \ldots, q = 5$ constraints just mentioned (max and min rebar separation, structural resistance efficiency, max/min rebar cross-section area, and neutral axis depth). For this case, there are two possible scenarios of

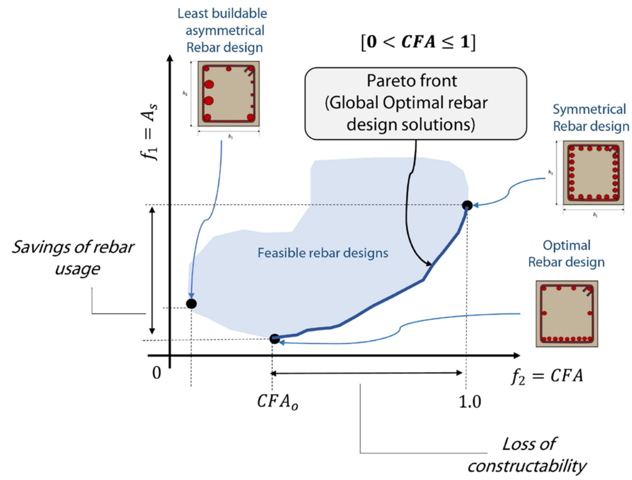

Fig. 8 Multi-objective Constructability-Based Optimization space of cross-section area for rebar designs in rectangular concrete columns

PF, as shown in Fig. 7. In the left panel, the best case scenario is depicted, in which the potential reduction of rebar material with asymmetrical optimal reinforcement is of such degree that at the end, the total construction costs are also considerably reduced. This, despite the reduction of constructability decreases and increase of the unit construction costs. However, the previous case might not always take place. Instead, a worst case scenario may be the situation, as shown in the right panel of Fig. 7, where the rate of decrease of constructability is higher than the rate of decrease of rebar usage, and in which, a symmetrical conventional design might actually have the lower total construction cost.

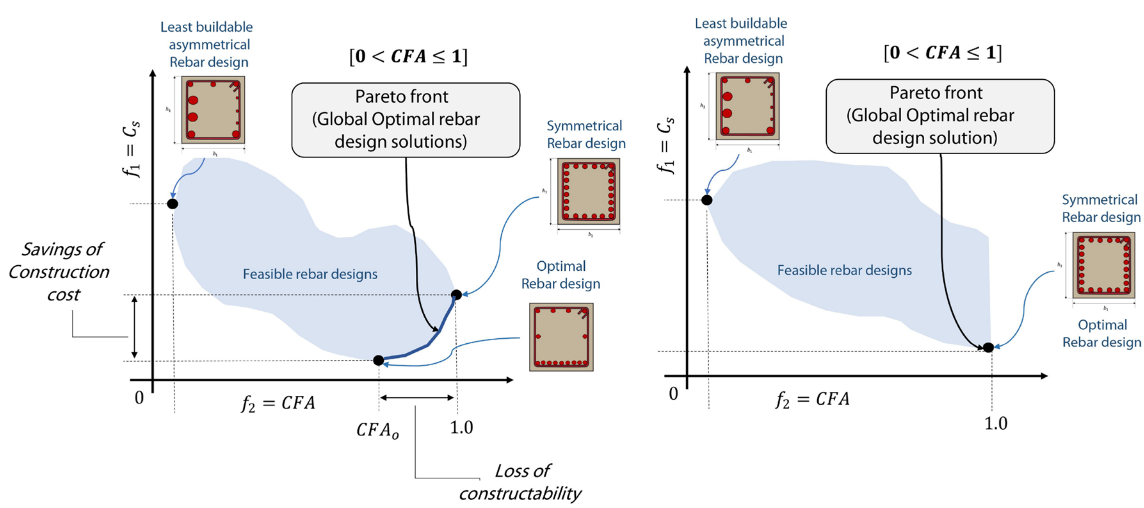

Fig. 7 Multi-objective Constructability-Based Optimization space of costs for rebar designs in rectangular concrete columns. Left panel: best case scenario. Right panel: Worst case scenario

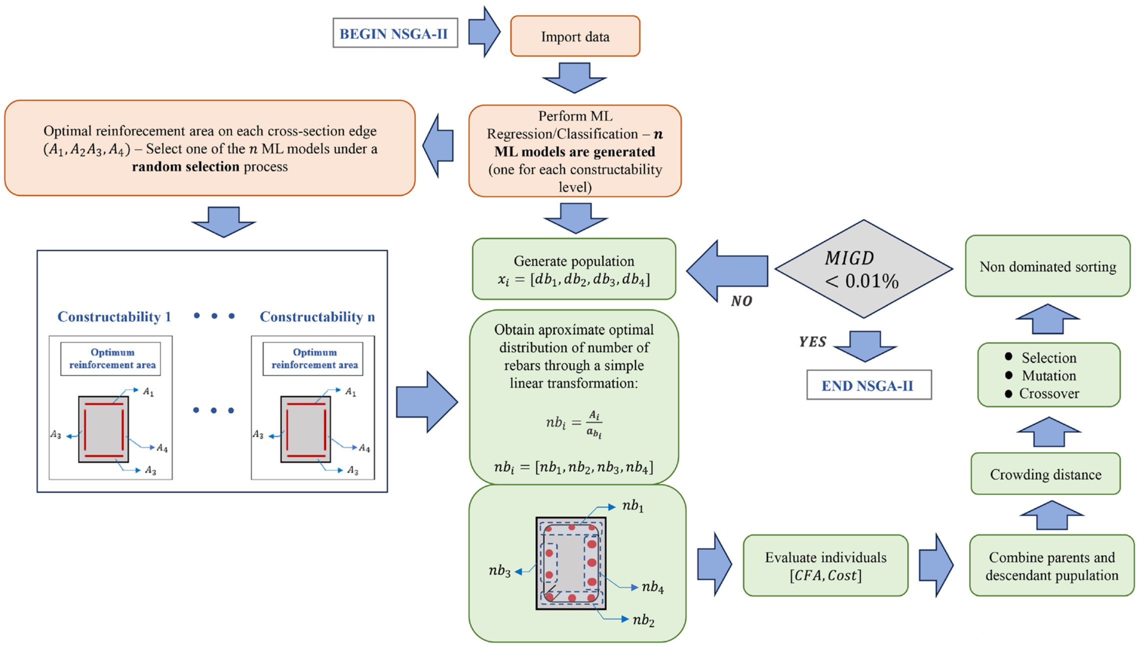

Fig. 9 Flow diagram of ML-Enhanced NSGA-II for Constructability-Based Multi-objective optimization of rebar design in columns

$$\begin{aligned}&\min[F(x) = (f_1(x), 1 - f_2(x))],\\&\text{S.T.: } x = [x_1, x_2, \ldots, x_n] \in S, \qquad .\\&\text{under: } g_i(x) \le y_i, \quad i = 1, 2, \ldots, q.\end{aligned} \tag{10}$$

On the other hand, when the problem is stated in terms of rebar usage, the objective function $f_1(x)$ in Eq. (10), would instead, represent the cross-section rebar area or rebar weight, which are linearly proportional. For this problem, it would, most likely, be the case for any column design, that a reduction of rebar area is generated with asymmetrical optimal designs in comparison to symmetrical conventional ones, as shown in Fig. 8.

3.5 Proposed algorithmic framework for MO optimization of rebar design in columns

The previously proposed general ML-Enhanced algorithmic framework shown in Fig. 5, based on decomposed optimization, could be adapted for any formulation, either for SO or MO optimization. For the MO formulation shown previously in Fig. 7, the NSGA-II of Deb et al. (2002) was used in this work. The algorithmic procedure with the ML enhancement is described as following in Fig. 9. It is to note, that for MO optimization more than one different optimum rebar design could be generated as output data, for better prediction of optimum PFs.

As it can be observed in this proposed framework, the meta-heuristic focuses entirely on the distribution of rebar sizes over the cross-section, without the need to initially restrict the number of rebars, as it had been proposed in previous related research. In Sánchez-Olivares and Tamas (2017), for instance, the number of rebar diameters were treated as optimization variables, and restricted manually at the beginning of the process. In Gil-Martín et al. (2010), such restriction was done by stating a double symmetry restriction of number of rebars over the cross-section (same number for the top and bottom faces and same number for the side faces). For the present proposed framework, ML models deal with such number of rebars, by considering the optimal amounts at each of the four cross-section faces from the generated data. This way, the higher the available number of commercial rebar sizes, the more advantageous the algorithmic framework becomes.

3.5.1 Step-wise description of the algorithmic framework

(1) Before any algorithmic process is started, the training of the ML model takes place. For this purpose, a database must be generated with the proposed data structure architecture shown in Fig. 10. This model, then, can be used for any column model to be optimally designed, and for as many as desired.

(2) For any particular column model, with its design loads, dimensions and materials, the ML model is used to predict the optimal reinforcement quantities at each cross-section edge, for all constructability-based optimum designs. These predicted values are saved and

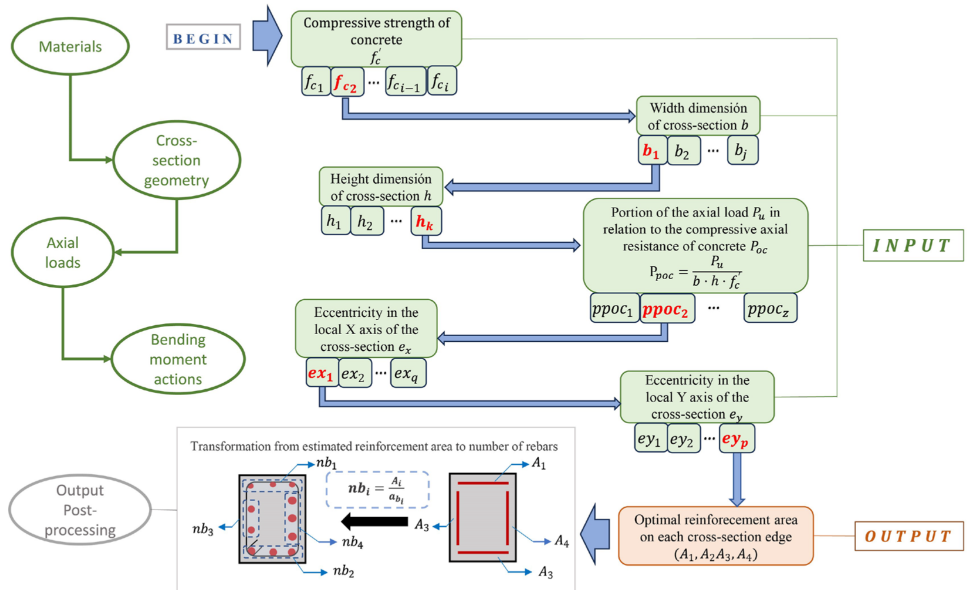

Fig. 10 Architecture of a tree-like data structure to train ML models for the estimation of optimal reinforcing steel area for any rectangular cross-section geometry, concrete and combination of biaxial bending loads

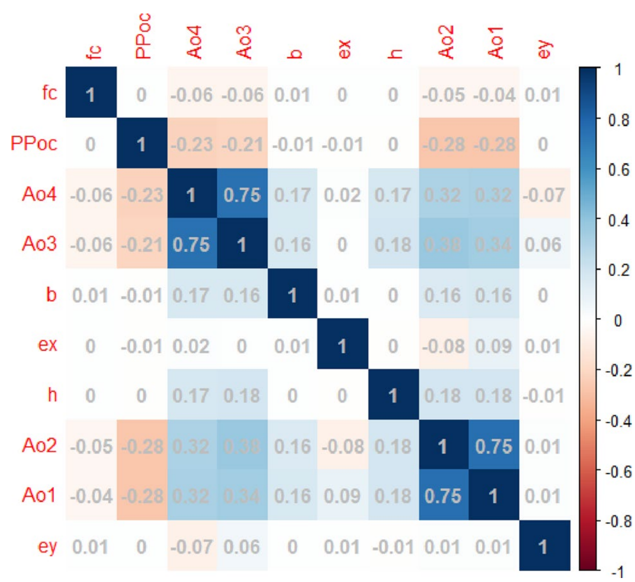

Fig. 11 Correlation analysis of training data features

used once the meta-heuristic optimization algorithm begins.

(3) The meta-heuristic algorithm is executed. For every potential design—combination of rebar sizes over the cross-section—the predicted values of optimal reinforcement quantities from the ML model are used to determine the optimal number of rebars at each cross-section edge. This computation is simply a linear transformation based on the corresponding rebar sizes, which have a respective cross-section area.

(4) The objective function(s) are computed for each potential design and the restrictions checked.

(5) The meta-heuristic optimization algorithm is then, finished, as for any other process, when a termination or convergence criteria is reached.

3.6 Data generation for ML training

A quite reliable option for the architecture of the data structures to be generated to train the ML models would be like the one in Fig. 10. Such data architecture consists of six main input variables related to the compressive strength of the concrete f_c', the cross-section dimensions b, h, the axial load P—in terms of the percentage of total compressive strength of the cross-section—and the load biaxial eccentricities e_x, e_y. The output variables on the other hand, would consist of four optimal reinforcement cross-section areas at each of the four column cross-section's edges. The correlation analysis of these variables with the output optimum areas is presented in Fig. 11. This way, for any combination of input variables of a column model an ML model would estimate the optimal distribution of required reinforcement quantity at each cross-section's edge. Then, for any combination of rebar diameter sizes at each cross-section's edge a simple linear transformation could be performed to determine the corresponding optimal combination of number of rebars to be placed, right after the ML model is executed. The training validation of the pure ML models is shown, in detail, in "Appendix 3."

To determine the optimal reinforcement cross-section quantities in a MO optimization fashion, a two-stage NSGA-II was used with the GA taking place in the second stage, instead of an ML model, as shown in Fig. 12. This way more than one constructability-based optimum designs can

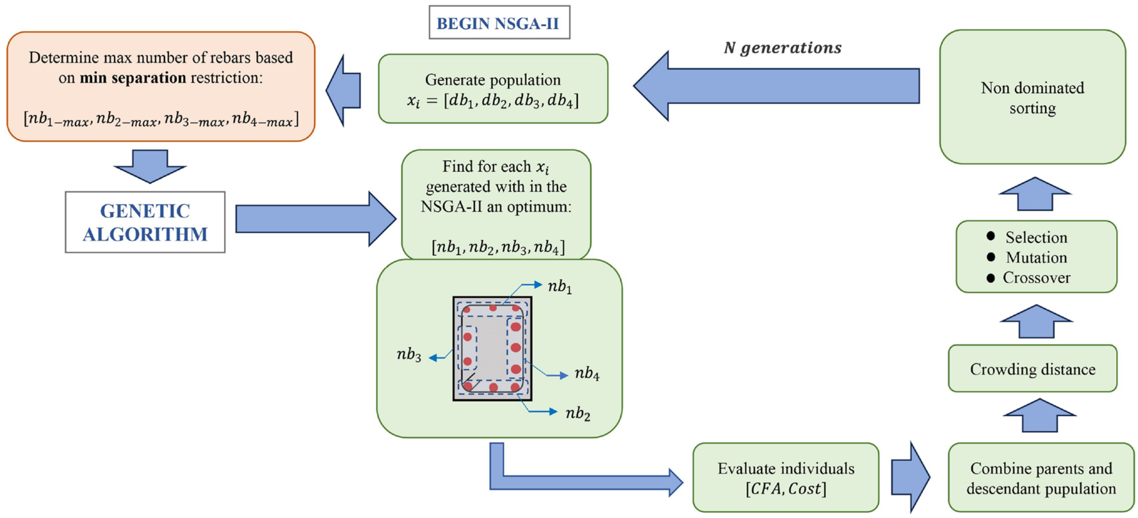

Fig. 12 Flow diagram of multi-objective optimization algorithm without ML enhancement with a two-stage NSGA-II for constructability-based rebar design in columns

Table 1 Considered commercially available rebar diameters

i-index	Rebar number (#)	Diam (in.)	Diam (cm)	Area (cm^2)
1	#4	0.500	1.270	1.266
2	#5	0.625	1.587	1.979
3	#6	0.750	1.905	2.850
4	#8	1.000	2.540	5.067
5	#9	1.125	2.857	6.413
6	#10	1.250	3.175	7.917
7	#12	1.500	3.810	11.400

Every rebar diameter has been assigned a respective index i according to its size

be extracted from the optimum PF to enhance the training data, making it more fit for MO optimization.

4 Results and discussion

4.1 Generation of training data

The data generated to carry out the following experimentation is done by considering the input variables' range shown in Fig. 13 with a Latin Hypercube Sampling LHS method. MATLAB software was used to carry out the experimentation. The commercial rebar diameters considered for the experimentations and data generation are shown as following

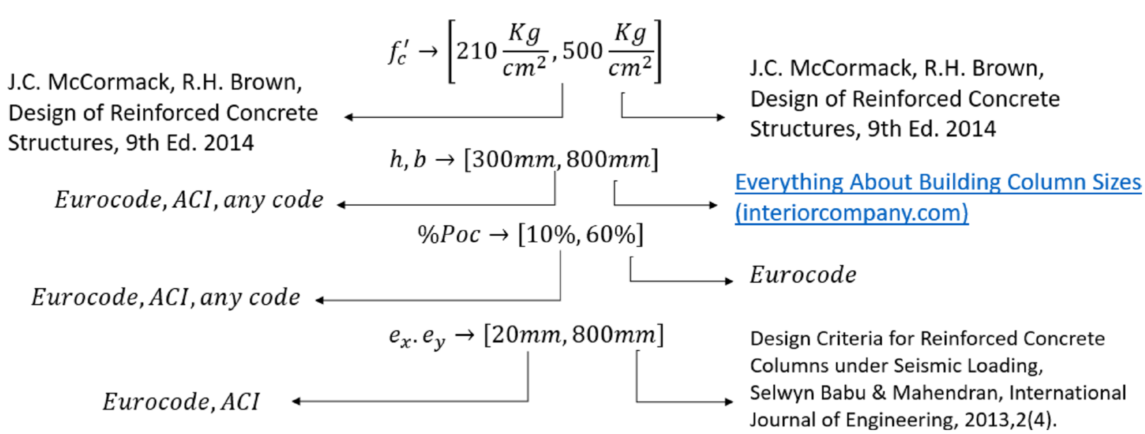

Fig. 13 Range of values for the input variables considered for data generation to train the ML-Enhanced meta-heuristic algorithms for the optimization design of rebar in concrete columns. See ACI (2019), Babu and Mahendran (2013), McCormac and Brown (2013), and European Union (2004)

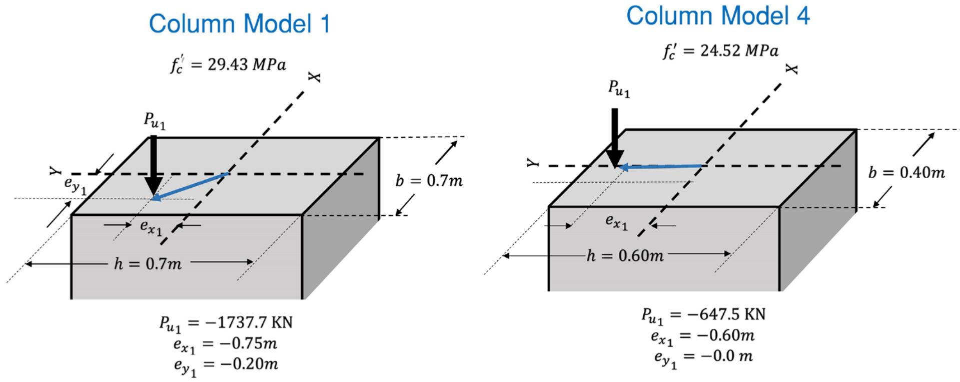

Fig. 14 Column models for experimentation of Constructability-Based MO optimization to demonstrate advantages of asymmetrical optimal rebar designs in relation to symmetrical ones, in terms of construction costs. (Left) Biaxial case. (Right) Uniaxial case

in Table 1. A concrete cover of 40 mm is considered. For MO optimization, only one constructability-based optimum designs from the optimum PF with the two-stage NSGA-II from Fig. 12 were extracted for a total of 10,000 samples. The generalization of performance of the ML-Enhanced Meta-heuristics is presented, in detail, in "Appendix 3." To assess such performance in a time efficient manner, a SO formulation was developed, in which Combinatorial Optimization (CO) was used for the output data generation with only one constructability-based optimum design as well, which results are shown in detail in "Appendix 4." The mathematical derivation of this CO formulation is described in detail in "Appendix 1" through the definition of certain boundaries to discretize the search space. The corresponding numerical complexity is showcased in "Appendix 2" for three different scenarios of commercial rebar availability in the market, by considering all the previously exposed design constraints by construction code.

4.2 Savings of rebar volumes and construction costs with optimal asymmetrical rebar through MO optimization

The decrease in constructability that asymmetrical designs may present in comparison to symmetrical ones is evident. However, the enormous portion of savings of rebar volumes that can be generated with optimal asymmetrical rebar in comparison to symmetrical designs can counteract such disadvantage, in such a degree, that at the end, the total construction costs might also decrease, considerably. To demonstrate this, the following column models of Fig. 14 were considered for experimentation through Constructability-Based MO Optimization, in terms of construction cost. The unit construction costs for any rebar design were computed based on the unit cost card shown in Table 2 parameterized with respect to the CFA. The weight factors required for the computation of the CFA according to (2) were considered as $W_{\text{unb}} = 0.5$ and $W_{\text{nd}} = 0.7$, in which there is no preference for the variability of number of rebars at each cross-section (see "Appendix 7" for more reference of these weight factors).

Table 2 Parameterized Unit Cost Card for rebar design of a rectangular concrete column based on constructability

Concept	Unit	Unit price	Quantity	Total $\frac{HKD}{\text{kg}}$
Materials				
Annealed wire Cal. 16, 1.59 mm diam.)	kg	$10.28\frac{HKD}{\text{kg}}$	0.04	0.4112
Rebar G-6000 of No. 3, ($\frac{3}{8}$diam), $0.557\frac{KG}{M}$	kg	$7.71\frac{HKD}{\text{kg}}$	0.105	0.81
Rebar G-6000 of Nos. 3 to 12, ($\frac{1}{2}$diam), $0.996\frac{KG}{M}$	kg	$7.71\frac{HKD}{\text{kg}}$	1.07	8.25
–		Subtotal materials		9.47
Manpower				
1 Iron worker and 1 Assistant	Workday	$1097.1\frac{HKD}{\text{Workday}}$	$\frac{1}{214.74\cdot\text{CFA}}\frac{Workday}{\text{kg}}$	$\frac{5.11}{\text{CFA}}$
–		Subtotal manpower		$\frac{5.11}{\text{CFA}}$
Tools and equipment				
Minor tolls	%	$\frac{5.11}{\text{CFA}}\frac{HKD}{\text{kg}}$	0.03	$\frac{0.1532}{\text{CFA}}$
–		Subtotal tools		$\frac{0.1532}{\text{CFA}}$
–		Unit cost		$9.47 + \frac{5.2633}{\text{CFA}}$

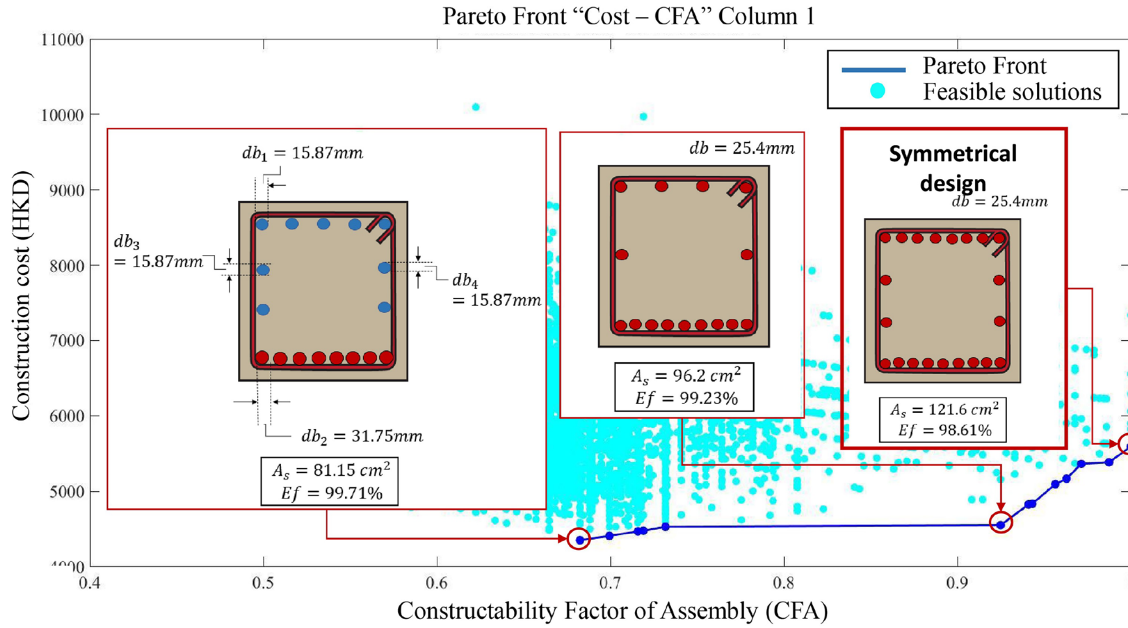

Fig. 15 Pareto front of optimal rebar designs obtained for column model 1. Cross-section dimensions: $b = 0.7$ m and $h = 0.7$ m

Fig. 16 Pareto front of optimal rebar designs obtained for column model 4. Cross-section dimensions: $b = 0.4$ m and $h = 0.6$ m

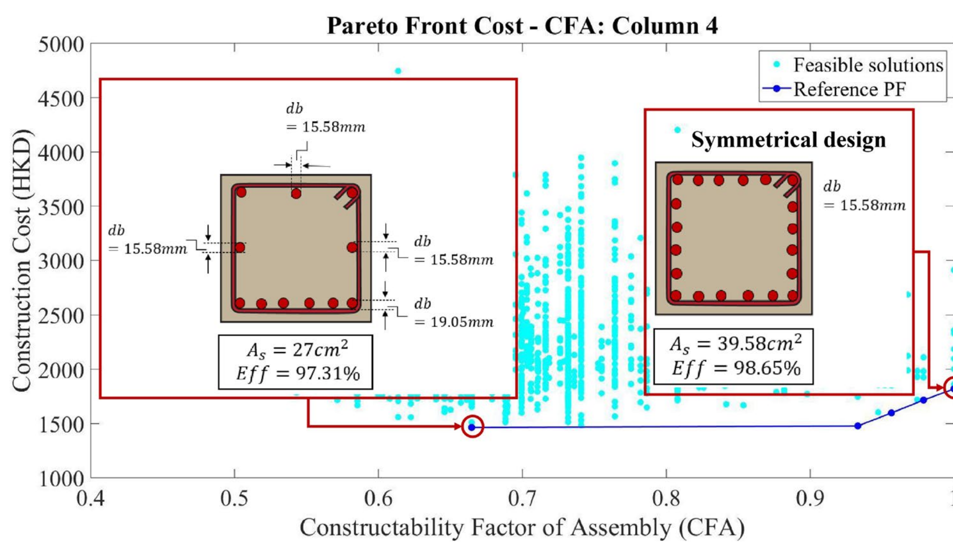

The resulting PFs are shown in Figs. 15 and 16. It can be observed in both PFs that despite of the decrease in constructability of the asymmetrical rebar designs, at the end, a great portion of those dominating optimal ones in the PF, turned out to have a considerably lower construction cost than symmetrical ones (up to 20% for the biaxial case and up to 18% for the uniaxial case). This is due to the great savings of rebar volumes that were obtained with those asymmetrical optimal designs. Even for the case of uniaxial bending, with more standardized cross-section dimensions, a great amount of cost savings were generated. In general, the asymmetry of the rebar distribution on the cross-sections follows the pattern of the governing resultant asymmetry of the load combinations. That is, for biaxial load combinations, the asymmetry of the rebar distribution will be, more likely, biaxial. And for uniaxial load combinations, the asymmetry of the rebar will be, more likely, uniaxial. Although in some instances, the rebar separation restriction might get in the way, as it was the case here for the biaxial load case.

It is worth to stress, also, that the density of the optimum PFs will depend greatly, on the BS model itself, that is, on the given weight factors. The less the asymmetry of

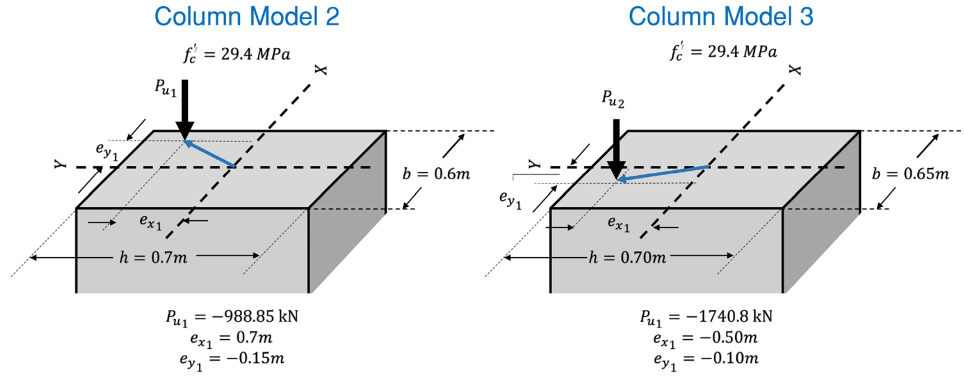

Fig. 17 Columns models considered for experimentation to assess the efficiency of the ML-Enhanced MO algorithms with the NSGA-II

Table 3 Algorithmic parameters for the NSGA-II algorithm

Scenario	NSGA-II
1	$N_{\text{population}} = 1500$
2	$p_{\text{mut}} = 0.25$
3	$\eta_{\text{crossover}} = 0.25$
4	$\eta_{\text{mut}} = 20$

Table 4 Algorithmic parameters for the GA into NSGA-II algorithm to determine a quasi-optimal PF of reference for each columns model of experimentation

Exhaustive Two-stage NSGA-II for PF of reference	Two-stage NSGA-II for performance comparison with ML-NSGA-II
$N_{\text{population}} = 80$	$N_{\text{population}} = 10$
$N_{\text{generations}} = 30$	$N_{\text{generations}} = 8$
$p_{\text{mut}} = 0.06$	$p_{\text{mut}} = 0.06$
$\eta_{\text{crossover}} = 0.65$	$\eta_{\text{crossover}} = 0.65$
$N_{\text{gemes}} = 80$	$N_{\text{gemes}} = 80$
$\text{Tournament}_{\text{selec}} = 0.8$	$\text{Tournament}_{\text{selec}} = 0.8$

the rebar distributions is penalized the more dense the PFs will be. This fact can be observed in the number of feasible solutions behind the previous optimum PFs. The less the CFA value, the more feasible solutions on display. This is because the complexity of number of asymmetrical designs is considerably larger than that for symmetrical designs, as demonstrated in "Appendix 1." Thus, when the asymmetry of rebar distribution is not that greatly penalized, the feasible solutions will shift to the right, closer to the symmetrical solutions, making the potential optimum PF of more density.

Analogous experimentations were carried out through SO optimization with CO, as shown in "Appendix 5." For such experimentations a larger sample of column models were assessed for a more proper data analysis. For these experimentations, different biaxial load cases of varying degree of asymmetry were considered. Even greatest findings were revealed in terms of construction cost and material savings and their relationship to the relative asymmetry of the multiple applied load combinations.

4.3 Efficiency of ML-Enhanced MO optimization algorithms

To showcase the efficiency of the ML-Enhanced MO optimization algorithms with the NSGA-II, in terms of time and convergence, the following two column models of Fig. 17 were considered for experimentation. For this purpose, to avoid the worst case scenario of a MO optimization formulation in terms of construction costs [as depicted previously in Fig. 7 (Right)], the MO optimization procedure was computed in terms of rebar area usage (total rebar weight, in this case) to ensure that a well-defined PF of reference was obtained, for comparison. For a more complete assessment of efficiency and accuracy of the ML-Enhanced algorithms, refer to "Appendix 4."

The parameters set for the NSGA-II are as in Table 3 for all ML enhancements. The Mean-Inverted Generational Distance (MIGD) was used for convergence criteria to terminate the iterations when MIGD < 0.01%. To better compute the MIGD, the construction costs were normalized. In this sense, to obtain an optimal PF of reference, the two-stage NSGA-II optimization process from Fig. 12 was used, with the parameters shown in Table 4 (Left). This way, an optimal combination of number of rebars, in terms of rebar usage, for each given individual generated (combination of rebar diameters) is determined. This same hybrid two-stage algorithm was used for performance comparison of time and convergence efficiency, in relation to the ML-Enhanced NSGA-II, although with different parameters for the GA, as shown in Table 4 (Right).

4.3.1 Convergence efficiency

The final PF obtained are shown in Figs. 18 and 19 for column models 2 and 3, respectively.

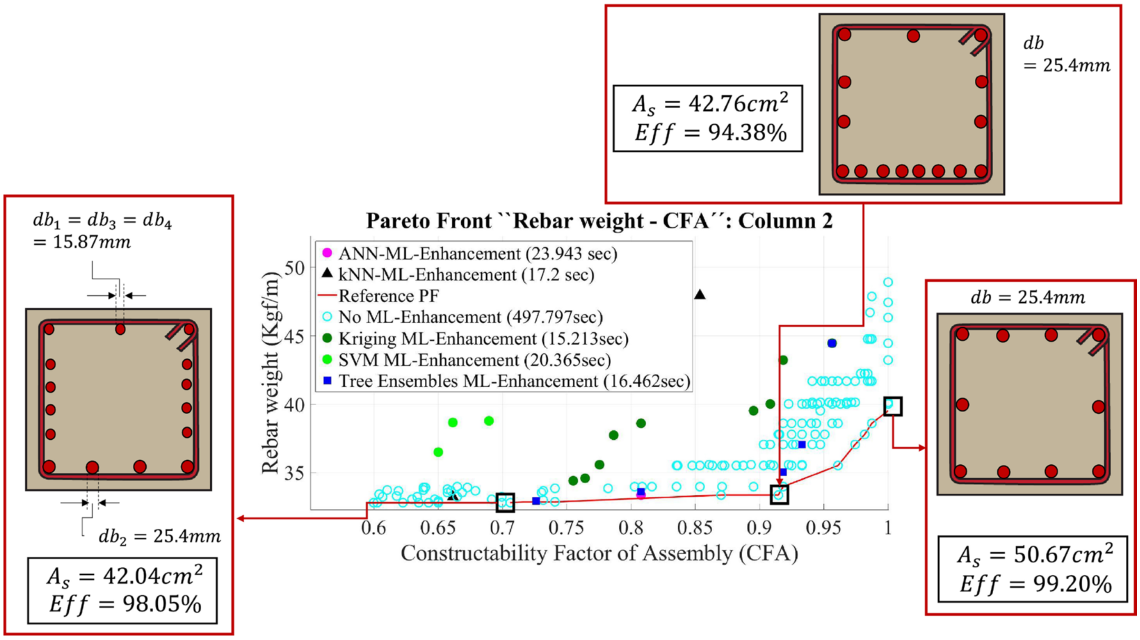

Fig. 18 Final obtained PF with each ML-Enhanced NSGA-II, for column model 2 of dimensions $b = 0.6$ m, $h = 0.7$ m

Fig. 19 Final obtained PF with each ML-Enhanced NSGA-II, for column model 3 of dimensions $b = 0.65$ m, $h = 0.7$ m

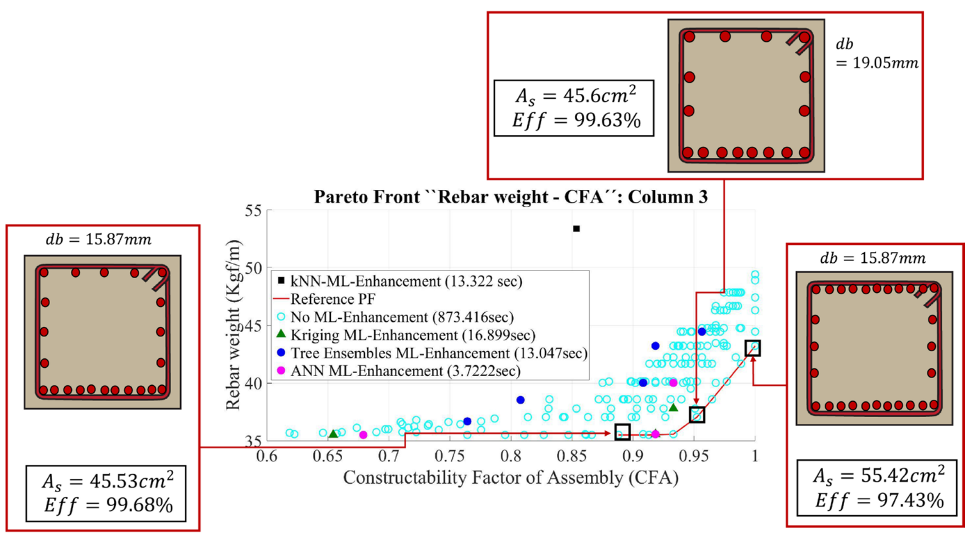

In summary, TE, ANN, and GP performed the better for ML enhancement, for both column models, both in time and convergence. However, for all cases, in general, TE was the best of all. An important factor of this is because of the tree-wise architecture of the learning data itself. The SVM and k-NN, on the other hand, performed the worst. The nonlinearity of multi-dimensional feature of the problem and the data itself make the SVM regression to perform the worst of all. As for the k-NN, even though its application has advantages in comparison to SVM for this problem, it enhances limited convergence performances. As it can be observed in their training/testing performance in Fig. 48, the models are just too simple to learn the complexity of the multi-dimensional tree-wise data and tend to overfit/underfit for new predictions. This increases the likeliness of the estimations to also be far away from the true optimal estimation of rebar area. The farther the estimation the more likely that less feasible solutions of rebar designs will be found. This can be observed in the previous results from Figs. 18 and 19, where the PF corresponding to the k-NN and SVM, are not even close to the optimal PF of reference. In Figs. 20 and 21, the evolution of the PF for column models 2 and 3, respectively, are shown. For column model 3, not even a single solution

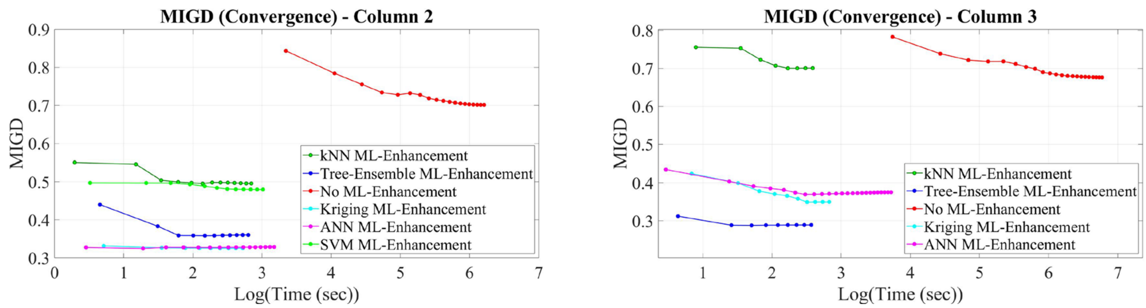

Fig. 20 Evolution of PF in time for each ML-Enhanced NSGA-II for column model 2. Top-Left: Tree Ensembles ML-Enhancement. Top-Right: Gaussian Process ML-Enhancement. Middle-Left: ANN ML-Enhancement. Middle-Right: *k*-NN ML-Enhancement. Bottom-Left: Non-ML-enhancement (GA NSGA-II). Bottom-Right: SVM ML-Enhancement

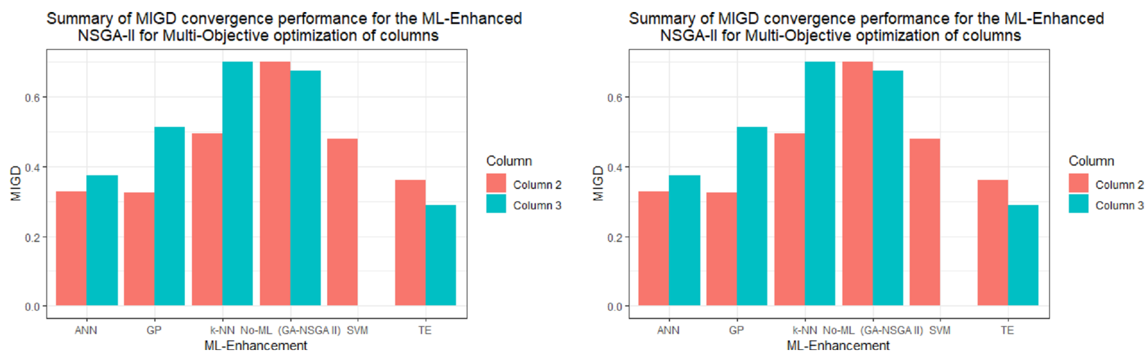

Fig. 21 Evolution of PF in time for each ML-Enhanced NSGA-II for column model 3. Top-Left: Tree Ensembles ML-Enhancement. Top-Right: Gaussian Process ML-Enhancement. Mid-Left: ANN ML-Enhancement. Bottom-Right: *k*-NN ML-Enhancement. Bottom-Left: Non-ML-enhancement (GA NSGA-II)

was found with SVM, meaning that the predictions were negative cross-section rebar areas.

As for the Non-enhanced NSGA-II, a great quality in regard of the PF convergence was obtained, both in density of solutions and convergence, in relation to the PF of reference, although in a much higher amount of time. This high demand of computational time of a Non-ML-enhanced meta-heuristic demonstrates the need of ML techniques to reduce it. The convergence in time per generation is depicted in Fig. 22. It can be observed that usually, for the algorithmic parameters just exposed, the ML-Enhanced NSGA-II would finish even before the Non-Enhanced NSGA-II completes one single generation. The results of both time efficiency and convergence are summarized in Fig. 23, for both column models, for better appreciation.

5 Conclusion

Several components of contribution were developed in this work. For the first time in the literature, a BS model for concrete columns was proposed through this research. In summary, the BS model turned out to be flexible and adaptive to any construction scenario. It was demonstrated that the development of these such models represent a novel and more accurate approach to assess the sensibility of any structural component of a infrastructure system with its respective construction cost.

A novel algorithmic framework based on decomposed optimization for the design of rebar in rectangular concrete columns was proposed in this work. It was demonstrated that under this framework, ML techniques can be deployed to aid meta-heuristic algorithms and reduce significantly the computational time demand to reach optimum solutions with quite acceptable performance levels of convergence. To demonstrate this, both SO and MO optimization algorithms enhanced with various ML models were developed and showcased.

To measure the general efficiency of the ML-Enhanced optimization algorithms, combinatorial optimization was used under a SO scenario as the comparison baseline, both for convergence and time performance, as shown in "Appendix 4." It was demonstrated that under this ML-based framework, the search space of rebar designs can be reduced to

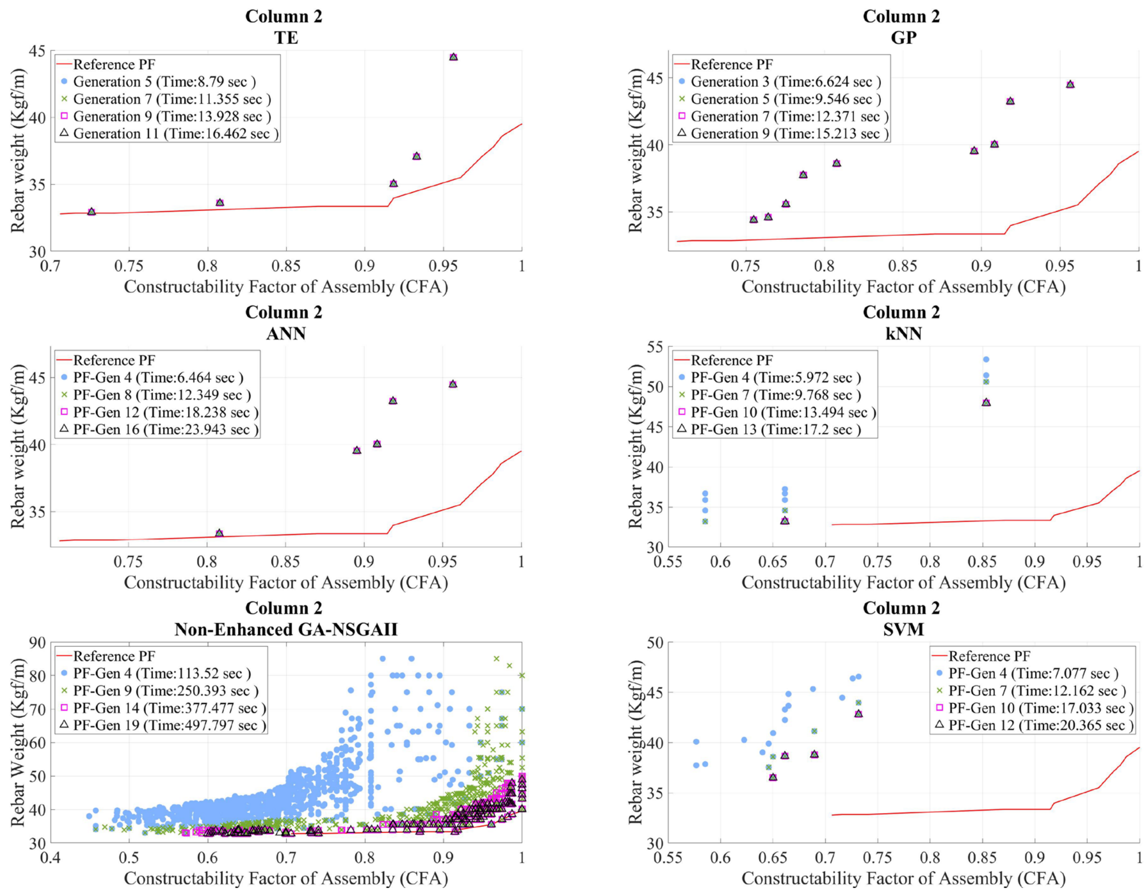

Fig. 22 Convergence of each ML-Enhanced NSGA-II in time in terms of the MIGD. Each dot represents a generation. Left panel: for column model 2. Right panel: for column model 3

proportions of no more than 2.5% and with levels of accuracy as high as 88% (Figs. 49 and 51).

For the last two showcased numerical models in the main part of the manuscript, under a MO optimization scenario, the ML-Enhanced algorithms demonstrated a reduction of execution time to proportions as small as 1.4% in relation to Non-ML-Enhanced algorithms, with even smaller convergence performance levels [less MIGD values Fig. 23 (Right)]. These benefits in time and convergence, however, were traded by sacrificing the density and uniformity of the optimal PF.

In all cases, for both SO and MO optimization process, Tree Ensembles had the best performance, in terms of convergence efficiency, followed by GP regression and ANN. In this sense, the use of the PSO as the Meta-heuristic was demonstrated to work better than the GA (Fig. 53). It was also demonstrated that the use of TE, GP, and ANN generates the best quality of PF, in terms of density and distribution, for MO optimization. In contrast, *k*-NN and SVM are not recommended to be used for these algorithmic frameworks, as their performance was, for all cases, the worst. These ML models tend to underfit and overfit the predictions of optimum rebar areas and thus, reducing their accuracy and increasing the MSE.

Additionally, it was demonstrated that the definition of BS models for rebar design are essential for complexity analysis of rebar design for RC elements through combinatorial optimization. It is through such complexity analysis that better assessment of performance can be carried out for SO optimization algorithms related to this problem.

Finally, it was demonstrated during the MO optimization experimentations, that indeed, considerable amounts of savings in material can be generated with optimal asymmetrical rebar designs in comparison to symmetrical ones. Savings of material of as much as 32% were observed for such experimentations. For these such savings of material usage, corresponding savings of constructions costs of as much as 20% were demonstrated to be enhanced, without significantly sacrificing the levels of constructability (see Figs. 15 and 16). In Figs. 18 and 19, savings of material usage of 17% and 18% were observed for column models 2 and 3, respectively. As for the SO optimization experimentations with CO, savings of material of as much as 72% were observed with similar amount of savings of construction costs of as much as 70%

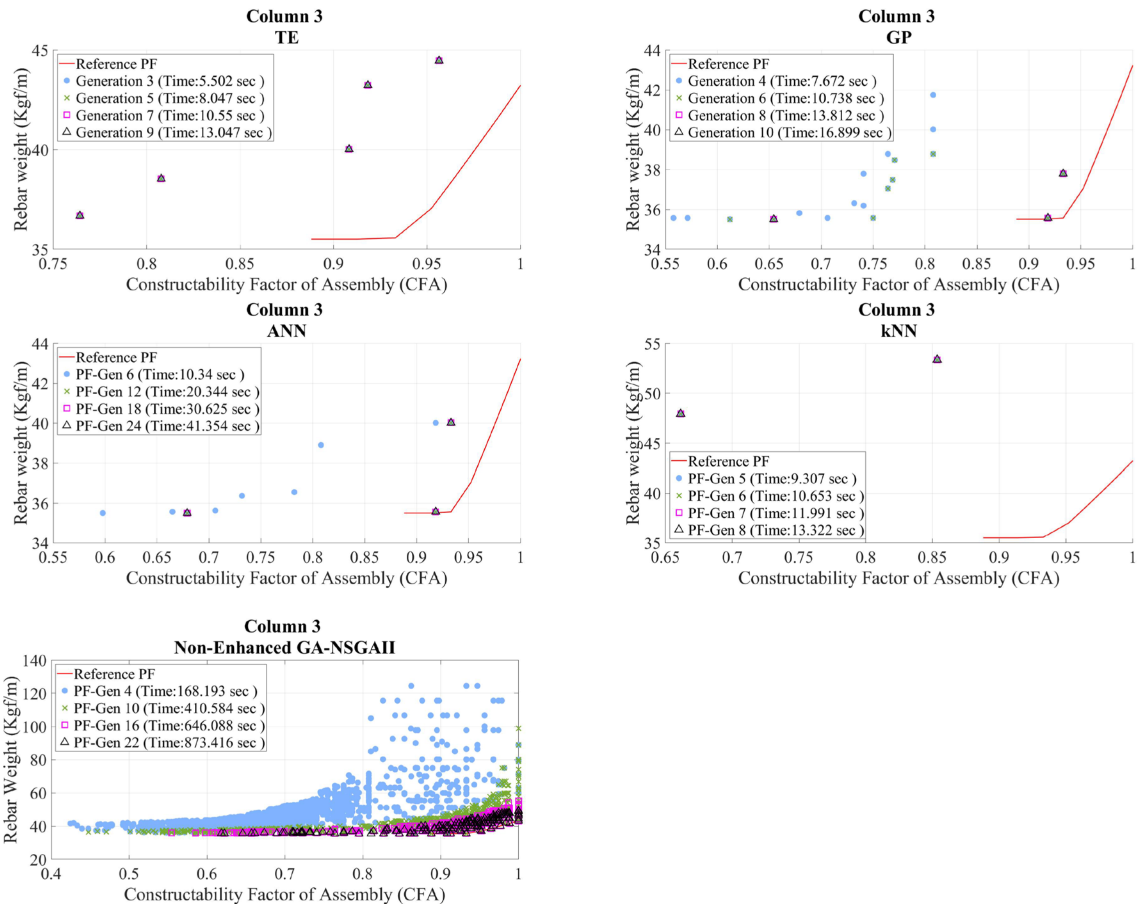

Fig. 23 Left panel: comparison of required execution time for each ML-Enhanced NSGA-II to reach the convergence termination criteria, for both column models of experimentation. Right panel: comparison of final MIGD convergence for each ML-Enhanced NSGA-II, for both column models of experimentation

(as shown in Fig. 55 of “Appendix 6”). Under this context, a proper parameter tuning of the weight factors for the BS models is preponderant to be carried out for each construction project at hand, for better estimation of construction costs of rebar designs.

5.1 Future work and limitations of this research

- Only one BS model was designed in this work for rectangular concrete columns. Further development of new BS models could be carried out, not only for rectangular concrete columns, but for any other structural element. This way, new Multi-objective Constructability-Based experimentations could be developed for each specific model and its respective applicable structural element, for a variety of problem cases. One potential problem case scenario, highly relevant nowadays, for instance, would be for CO_2 emission optimization for RC structures. To integrate BS models into this sort of problems, a more comprehensive relationship between the potential carbon footprint of optimal structural designs and their associated construction cost could be estimated, based on more proper constructability measurements.
- Up to this day, the existing metrics of constructability through BS models for RC buildings do not consider the quality of the reinforcement detailing, neither at the element nor at the building level. With the development of new BS models for other types of structural elements, on a local system of reference, such as the one here developed for columns, the formulation of BS models at the building level on a global system of reference could be developed. Such BS models could complement the existing ones that only consider the element’s dimensions and overall geometry of the structures.
- When adapting and extending this algorithmic framework to other structural elements, two main aspects must be considered: (1) to adapt the learning data architecture (used to train the ML part of the optimization process) to the mechanical behavior of the element in question, so that biaxial/uniaxial bending may be considered and/or shear and axial loads and (2) to adapt the meta-heuristic part (focused on the distribution of rebars) to the design

mechanism of the element, that is, considering one, two or three cross-sections to be designed simultaneously based on free clash detection.

- The demonstrated levels of accuracy of the algorithms of approximately 90% entails that they would not produce acceptable design solutions or no solution at all for approximately 1 out 10 column models, when, in fact, there might be acceptable solutions for such model. To mitigate this drawback, it is recommended to build the TE, ANN, and GP regression model before any optimization design and use the one that gives the better solution for each design at hand. This way, in case no output design is generated by one ML model for a specific column, there is a 90% probability that the other ML model will, indeed, provide an acceptable solution for such column.

Appendix 1: Breakdown of combinatorial formulations of rebar design under the constructability model

The following combinatorial formulations serve as basis for the computation of the rebar space complexity (described in detail in "Appendix 2") under the hereby defined constructability model.

A.1 Max number of symmetrical conventional possibilities of reinforcement

From the rectangular cross-section of Fig. 24, it is easy to determine the max number of rebars of diameter db that can be fit into the width allowed space ($b - 2\text{cover}$) of a rectangular cross-section separated between each other by a minimum separation (sep_{min}) as (11):

$$\text{nmaxb}_{\text{bars}} =_{\text{roundLower}} \left(\frac{b - 2\text{cover}}{\text{sep}_{\text{min}} + \text{db}} \right) + 1. \tag{11}$$

Now, the min number of rebars that should be placed over a rectangular cross-section boundary is 2 (defined by codes to assure a good confinement), then the max number of reinforcement possibilities for a rebar diameter db would be given by (12), which could be transformed to (13) when substituting $\text{nmaxb}_{\text{bar}}$ of equation (24) in it:

$$N_i^{\text{basic}} = \text{nmaxb}_{\text{bars}} - 2 + 1 \quad , \tag{12}$$

$$N_i^{\text{basic}} =_{\text{roundLower}} \left(\frac{b - 2\text{cover}}{\text{sep}_{\text{min}} + \text{db}} \right) \quad . \tag{13}$$

Such quantity of number of evaluations $\text{Neval}_{\text{max}}$ would apply to every available rebar diameter i in consideration (see Table 1), so that the total number of evaluations would be the sum of (13) for each rebar diameter (changing the value db for its respective db_i).

$$N_{\text{eval-max}}^{\text{basic}} = \sum_{i=1}^{i=n} N_i^{\text{basic}}. \tag{14}$$

A.2 Max number of symmetrical non-conventional possibilities of reinforcement

This previous reinforcement formulation could be adapted for the case in which two rebar diameters were allowed to be placed over a cross-section such that only the opposite boundaries would be reinforced with the same rebar diameter. This corresponds to a combinatorial problem in the form $V_m^n = m!/(m-n)!$, where m would denote the number of possible rebar diameters to choose from and n the number of the different rebar diameters allowed ($n = 2$). Note that such expression could be also expressed as $V_m^n = m^n - m$. To illustrate this fact let us assume that a rebar design in individual rebar sets of a diameter index $i = 2$ from Table 1 has been performed. In order to assure that the restriction sep_{min} is complied in every rebar combination, then only smaller rebar diameters could be exchanged with the already existing one i (that is, only rebar diameters of index $i = 1$ and $i = 2$ could be used). Therefore, the number of combinations

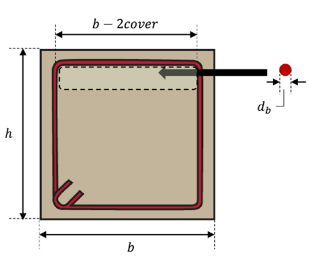

Fig. 24 Rectangular concrete cross-section used to illustrate the how to determine the max number of rebars that could bi fitted horizontally along the upper/lower cross-section's boundaries

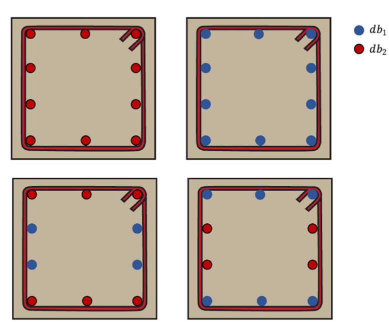

Fig. 25 Set of rectangular concrete cross-sections symmetrically reinforced to illustrate the number of symmetrical designs combinations that could be generated with only two rebar diameters

could be computed as $i^2 = 2^2 = 4$ (see Fig. 25). However, the rebar designs with only one rebar diameter have already been evaluated, thus only two additional evaluations would take place, a quantity that could have been determined as $V_i^2 = i!/(i-2)! = i^2 - i = 2^2 - 2 = 2$ (which would apply for every design of diameter index i). This way, the total number of max evaluations to carry out for this reinforcement option would be determined by multiplying the number of evaluations from Eq. (13) by the factor $(1 + (i^2 - i))$, applied and added up for every diameter index i as in (15).

$$N_{\text{eval-max}} =_{\text{roundLower}} \left(\frac{b - 2\text{cover}_x}{\text{sep}_{\min} + \text{db}_i}\right)\left(1 + (i^2 - i)\right). \tag{15}$$

A.3 Max number of asymmetrical non-conventional possibilities of reinforcement

There is the possibility to extend the previous formulation of symmetrical non-conventional designs to asymmetrical ones. By considering that as many as four rebar diameters could be placed over the cross-section. Then, to define the max number of design evaluations, Eq. (15) could be rearranged by only modifying the term $(i^2 - i) \rightarrow (i^4 - i^2)$ given that for this reinforcement option as many as four different rebar diameters are allowed to be placed simultaneously over the cross-section. Therefore, the max number of evaluations for a given asymmetrical rebar design from this prototype would be determined as (16), where i is the rebar diameter index. Note that the term $i = 2$ in the equation refers to the exclusion of those symmetrical rebar designs. Figure 26 illustrates this combinatorial formulation by considering $i = 2$.

$$N_{\text{eval-max}} =_{\text{roundLower}} \left(\frac{b - 2\text{cover}_x}{\text{sep}_{\min} + \text{db}_i}\right) \cdot (i^4 - i^2). \tag{16}$$

Another alternative for an asymmetrical reinforcement that may take place from a basic conventional symmetrical design is with a homogeneous rebar diameter distributed asymmetrically over a cross-section, for which the max total number of evaluations for each symmetrical option could be determined as (17). Where nb_b and nb_h is the number of rebars at the upper/lower cross-section boundaries and at right/left cross-section boundaries, respectively. Note that

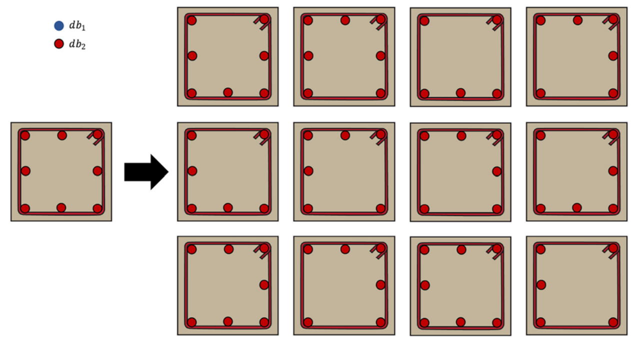

Fig. 27 Potential combinations of asymmetrical rebar arrangements from a symmetrical rebar design for a rebar design of the reinforcement prototype **Asym1Diam**

$\text{nb}_\text{b} \geq 2$ must be always complied according to design codes. Figure 27 illustrates this case for $\text{nb}_\text{b} = 3$, $\text{nb}_\text{h} = 1$, and $i = 2$.

$$N_{\text{ev-max}}^{\text{non-conv}} = (\text{nb}_\text{b} - 1)^2(\text{nb}_\text{h} + 1)^2 - (\text{nb}_\text{b} - 1)(\text{nb}_\text{h} + 1) \quad , \tag{17}$$

$$N_{\text{ev-max}}^{\text{non-conv}} = (3 - 1)^2(1 + 1)^2 - (3 - 1)(1 + 1) = 12 \quad . \tag{18}$$

Now, let us imagine that for each design from the previous formulation of a homogeneous rebar diameter, new designs could be generated by only mutating the rebars' diameter so that a max of four rebars diameters could be simultaneously placed over the cross-section (one diameter for each cross-section boundary). Thus, a new rebar design prototype could be generated by mixing the previous one with the design prototype corresponding to a max of four rebar diameters, so that the rebars could be placed asymmetrically both in number and in rebar diameters. Hence, for this case, the max number of evaluations for each asymmetrical design of the previous reinforcement prototype could be determined as (19), in which only the combinatorial term $(i^4 - i)$ has been added:

$$N_{\text{ev-max}} = [(\text{nb}_\text{b} - 1)^2(\text{nb}_\text{h} + 1)^2 - (\text{nb}_\text{b} - 1)(\text{nb}_\text{h} + 1)] \cdot (i^4 - i). \tag{19}$$

Figure 28 illustrates this case for $i = 2$ from Table 1), by taking the top-left rebar design from Fig. 27, so that its possible number of rebar permutations is $i^4 - i = 2^4 - 2 = 14$:

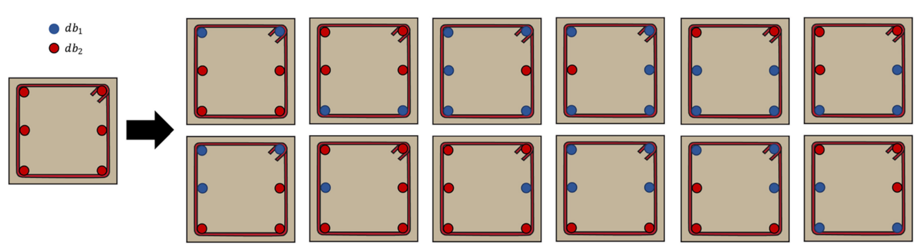

Fig. 26 Potential combinations of asymmetrical rebar arrangements from a symmetrical rebar design for the reinforcement prototype **Asym-Sym4Diam** by considering $i = 2$

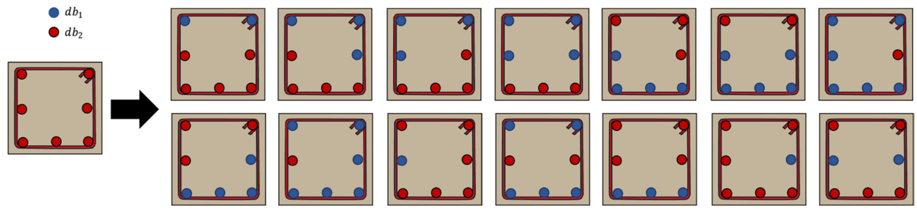

Fig. 28 Potential combinations of asymmetrical rebar arrangements from an asymmetrical rebar design of the prototype **Asym1Diam** from which the reinforcement prototype **Asym-4Diam** takes place

A.4 Assembly of sample sub-spaces of rebar designs

All the previous sub-sample formulations for the optimal design of rebar could be assembled into only one sub-sample, to take the most advantage of each loop and reduce the number of iterations or evaluations required to traverse through the whole set of potential solutions. In such both subsamples, either asymmetrical or symmetrical rebar designs may take place. For this such case, the counting formula of max evaluations is given by (21), where N_i^{sym} is defined as follows (20):

$$N_i^{\text{sym}} = \text{roundLower}\left(\frac{b - 2\text{cover}}{\text{sep}_{\text{min}} + \text{db}_i}\right) \quad , \tag{20}$$

$$N_{\text{ev-max}}^{\text{1pack-assem}} = N_{\text{ev-max}}^{\text{basic}} \cdot \left[i^4 + \sum_{j=1}^{N_i^{\text{sym}}} ((\text{nb}_{\text{bj}} - 1)^2 (\text{nb}_{\text{hj}} + 1)^2 \right. \cdot$$
$$\left. - (\text{nb}_{\text{bj}} - 1)(\text{nb}_{\text{hj}} + 1)) \cdot (i^4 - i) \right] \tag{21}$$

Appendix 2: Numerical analysis of rebar complexity under the constructability model

B.1 Sub-space characterization of buildable rebar design

The construction of a BS model makes it possible to execute a complexity analysis of rebar designs. Based on the restriction ND ≤ 4, it is possible to estimate the max number of constructible design solutions through discrete combinatorial, as described in "Appendix 1". The process to carry on such combinatorial evaluations starts from a very primal optimal symmetrical design composed of only one rebar diameter. This primal optimal basic design takes place by making a first reduction of the search space based on the design constraints corresponding to the max and min reinforcement cross-section area (3) and the structural efficiency demand 5. For this purpose, the Idealized Smeared Reinforcement (ISR) analogy (Verduzco et al. 2022), is used as shown in Fig. 29 in which the reinforcement is simulated as reinforcing steel laminates of uniform

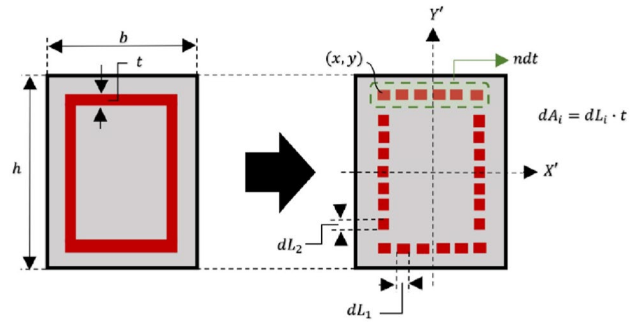

Fig. 29 ISR analogy to simulate reinforcement for concrete column of rectangular cross-section

thickness uniformly distributed over the cross-section's boundaries.

This way, a max number of rebars can be determined for any given rebar diameter size so that $A_{\text{bars}} \leq A_t(t)$ as shown in Fig. 30. Then, a combinatorial optimization approach takes place to determine the optimal distribution of such rebars over the cross-section. This basic combinatorial optimization process was demonstrated in (14) of "Appendix 1" to be of linear complexity $O(b)$.

From this point on, any different possible design derived from it is created by permuting either the number of rebars or the diameter at each cross-section boundary. Such permutations can be grouped according to a certain pattern distribution of number of rebars or diameters at the boundaries.

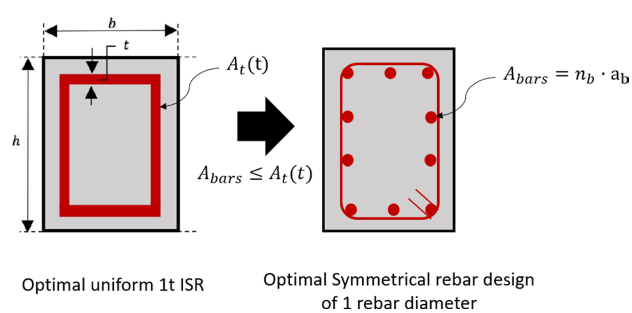

Fig. 30 Transformation from an optimal ISR to an optimal basic design of rebar composed of only one rebar diameter

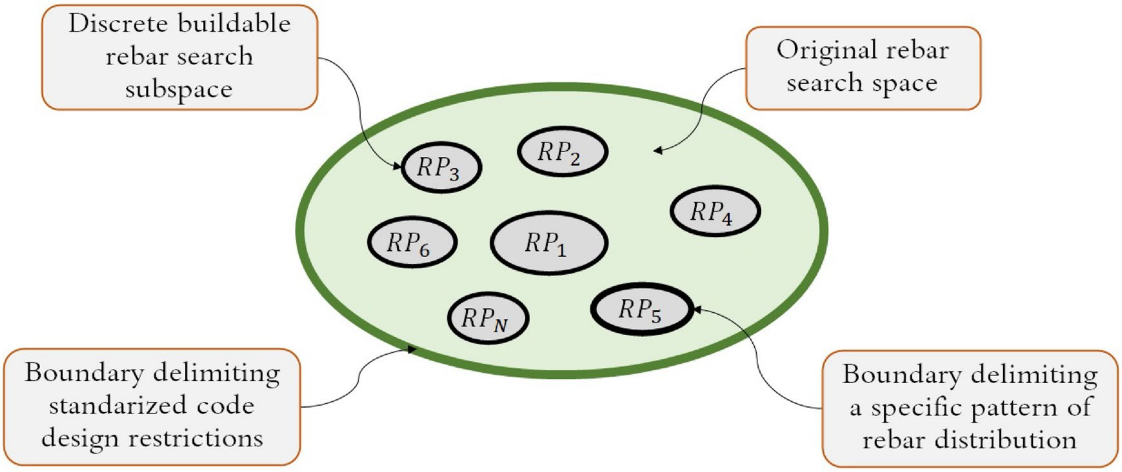

Fig. 31 Depiction of a set of discrete search sub-spaces representing different rebar design prototypes

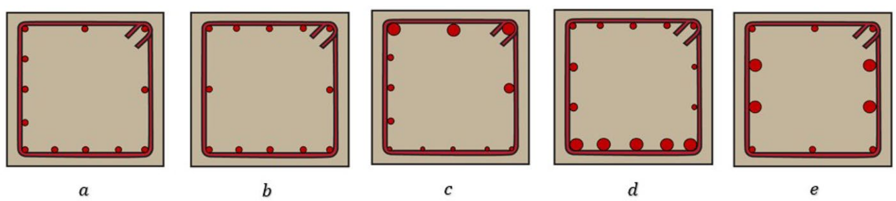

Fig. 32 Alternatives of reinforcing bar designs for rectangular column's cross-sections in individual rebars. **a** RP consisting of only one rebar diameter with an asymmetrical distribution of number of rebars, **b** RP consisting of one rebar diameter with a symmetrical distribution of number of rebars (most basic symmetrical design), **c** RP consisting of a max of four rebar diameters with an asymmetrical distribution of number of rebars, **d** RP consisting of a max of four rebar diameters with a symmetrical distribution of number of rebars, and **e** RP consisting of a max two rebar diameters with a symmetrical distribution of number of rebars

This grouping of patterns gives way to what is called here a *Rebar Prototype (RP)*[1], as depicted in Fig. 31. Thus, the sum of all possible rebar patterns derived from a very basic symmetrical design would represent the whole search space of rebar designs in question. Each RP, then, would represent only a discrete sub-space set of design solutions.

In summary, five different RP's were identified for the whole search space of constructable design outcomes, as shown in Fig. 32.

B.2 Complexity analysis of rebar design

When designing an algorithm there are two main issues to consider the correctness of the algorithm (that the algorithm performs the desired task correctly) and the complexity of the algorithm (how fast is the algorithm and how do the number of required computations grow as the input data grows). For the latter issue, time complexity is the most common approach used in computational science, although memory space or simply the number of basic representative operations might also be important, for which a *Worst case complexity estimate* or in many cases an *Average worst case complexity estimate* may be of great relevance. In this case, we are interested in computing how fast does the size of each RP sub-space grows as the column cross-section grows in dimension, so that when a new optimization algorithm is developed it would be possible to estimate the time efficiency for optimum convergence in relation to the average number of potential solutions.

Table 5 Scenarios of commercial rebar availability for the assessment of rebar designs complexity

Scenario	Commercially available rebars (*i*-index)
1	1, 2, 3, 4, 5, 6, 7
2	1, 3, 4, 5, 7
3	1, 3, 4

[1] A rebar geometrical configuration that follows a certain pattern and complies with certain restrictions, such as number of different rebar diameters, spacing between rebars, and symmetry

Table 6 Resume of numerical sample sub-space size complexity for rebar designs in individual rebars and in packages of two in rectangular cross-section columns

Scenario	Rebar sub-space Complexity $O(g(b))$
1	$O(e^{f(b)})$
2	$O(e^{f(b)})$
3	$O(e^{f(b)})$

For this purpose, the cross-section dimension b could be considered as the parameter of reference, given that for any case, it would be smaller than the height dimension ($b \leq h$) and therefore, it would govern the potential number of rebar designs. Of course, such complexity would also be in function of the available commercial rebars. For this reason, it is important to assess different scenarios of commercial availability of rebars to come up with a better complexity estimate. Nowadays, innumerable diameters sizes and grades of steel reinforcing bars can be found in the market all around the world. For any reinforced concrete project at hand it is crucial to analyze the surrounding market way before the early design stages. In North America, for instance, it is common to find even more than 10 rebar diameter sizes, for which a huge rebar design solution space corresponds. A numerical complexity analysis of buildable rebar design is showcased next for three different scenarios of rebar availability, as shown next in Table 5, in which the rebar indices of all the possible rebar diameters from Table 1 are listed.

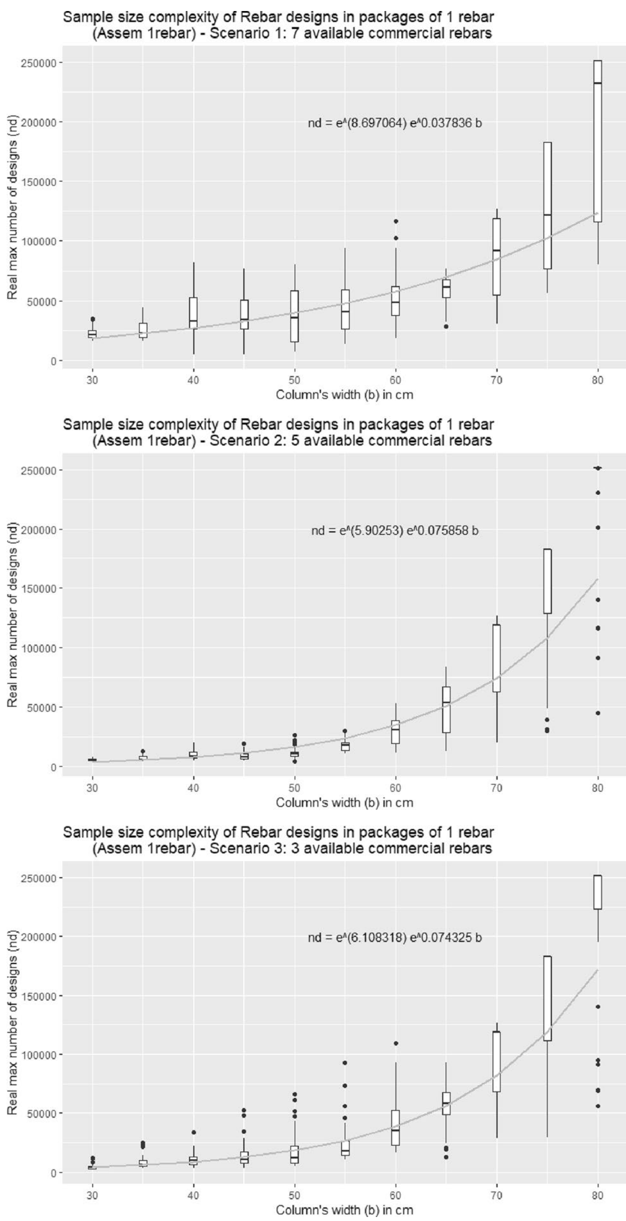

Fig. 33 Real number of representative rebar design evaluations as b increases, for 3 different cases of commercial rebar availability

In practice, however, given the design constraints set by design code specifications the real sample size of feasible rebar designs is much more reduced than the original theoretical combinatorial one, as shown next. The same design constraints by code specifications from the ACI-318-19 shown previously in (3), (4), and (5) concerning the max and min reinforcement area quantities, rebar separation, and the resistance efficiency, respectively, were used for this analysis.

The experimentations were carried out by executing 40 runs for each commercial rebar availability scenario, each run consisting of 11 cross-section models ranging in cross-section width dimensions b in increments of 0.05m from a minimum dimension of 0.3m and a max of 0.8m. For each cross-section dimension a set of asymmetrical biaxial load combinations in pairs would be generated randomly with a uniform distribution from the ranges in (22):

$$\begin{aligned} &P_u \in \mathcal{U}[-1226.25\,\text{kN}, -117.72\,\text{kN}], \\ &\text{Mu}_{x_1}, \text{Mu}_{y_1} \in \mathcal{U}[147.15\,\text{kN m}, 1520.55\,\text{kN m}], \\ &\text{Mu}_{x_2}, \text{Mu}_{y_2} \in \mathcal{U}[-1520.55\,\text{kN m}, -147.15\,\text{kN m}]. \end{aligned} \tag{22}$$

Once the data were gathered, linear regression was deployed to assess such complexity. The results are shown next in Fig. 33 and resumed in Table 6 in terms of complexity in asymptotic notation $O(g(b))$, in which it can be observed that the complexity growth is best characterized by exponential functions, for all scenarios:

Appendix 3: Validation of pure ML models training for enhancement

C.1 Validation of pure ML models for enhancement

The tuned parameters and testing/training validation, specifically for the data size of $N = 10{,}000$ samples used for the shown-case column models, are presented next, for

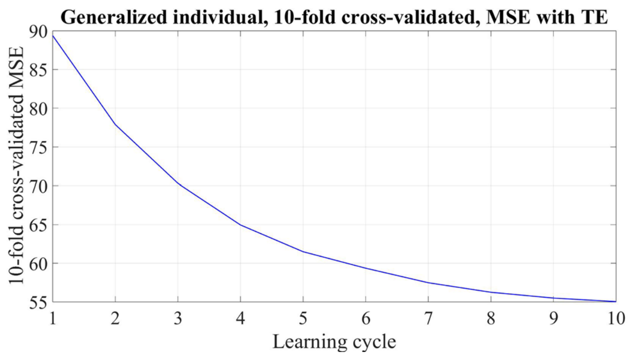

Fig. 34 Cumulative MSE in function of number of learning cycles of Optimized Boosting TE

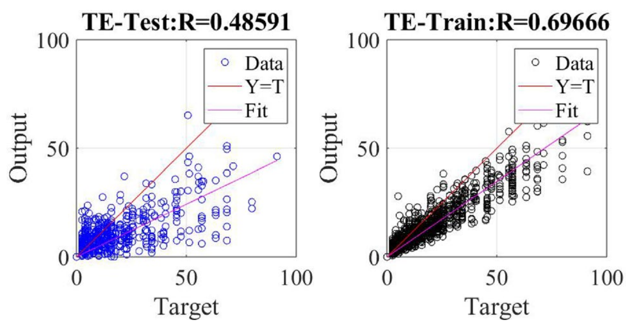

Fig. 35 Regression coefficient, in terms of rebar cross-section area (cm^2), for optimized Boosting TE

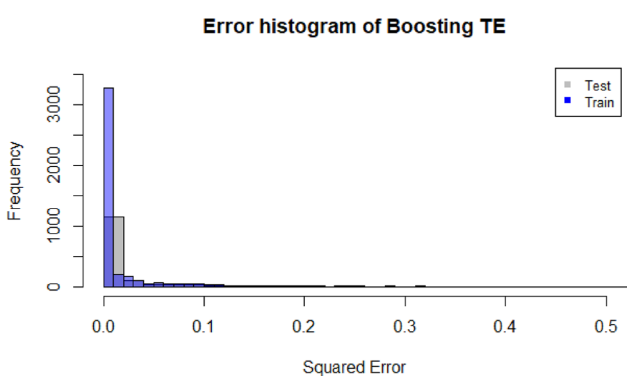

Fig. 36 Error histogram for optimized Boosting TE

the pure ML models used for enhancement. For this purpose, tenfold cross-validation was deployed to optimize the hyper-parameters for each model. The results here exposed can be related later to the general efficiency of the ML-Enhanced Meta-heuristics.

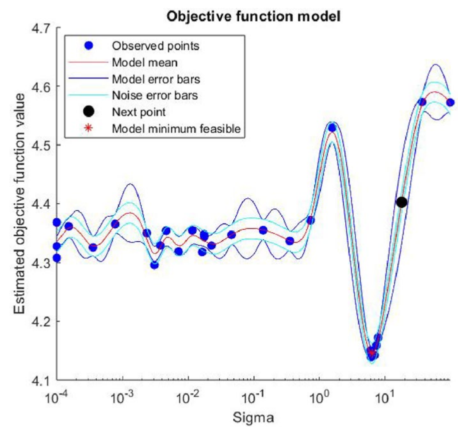

Fig. 37 Hyper-parameter optimization for Gaussian Process regression model

C.1.1. Tree Ensembles

- Least Squares boosting is used.
- One hundred trees compose the ensemble.
- The tree depth is composed of 5 for Minimum Leaf Size and 10 Minimum Parent Size.
- Bayesian optimization was used to find the following optimal hyper-parameters of the TE model:
  - A max of 1683 splits compose the ensemble.
  - Learning rate equal to 0.1788.
  - Number of learning cycles equal to 10.
  - The estimation of generalization MRE error is shown next for each learning cycle (Fig. 34).

The regression coefficient results and error histograms, with the previous optimized TE, are shown below (Fig. 35, 36), respectively:

C.1.2 Gaussian process regression

For Gaussian Process regression, a Squared Exponential kernel function was used. After having performed Bayesian Optimization, the optimum σ value obtained was $\sigma_{opt} = 6.1302$, as shown next for 30 function evaluations (Fig. 37). The corresponding regression coefficients and error histograms with the optimized model are shown in (Fig. 38, 39), respectively:

1.1.3 Artificial neural networks

Back-propagation ANN were used with the following initial parameters:

- Hidden layers equal to 10.
- *N* layers equal to 11.

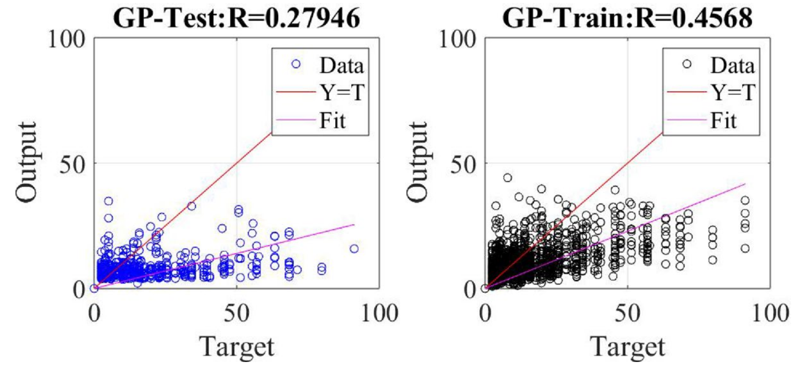

Fig. 38 Regression coefficient, in terms of rebar cross-section area (cm^2), for optimized GP regression model

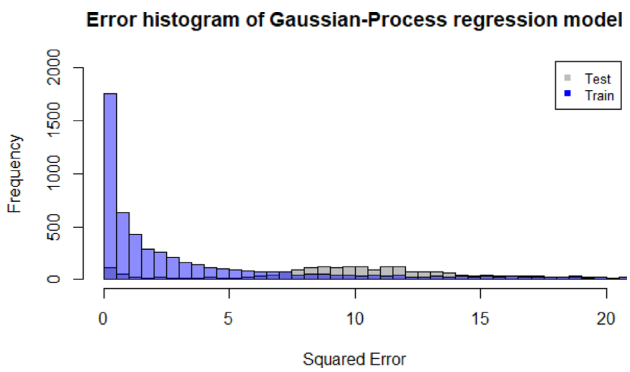

Fig. 39 Error histogram for optimized GP regression model

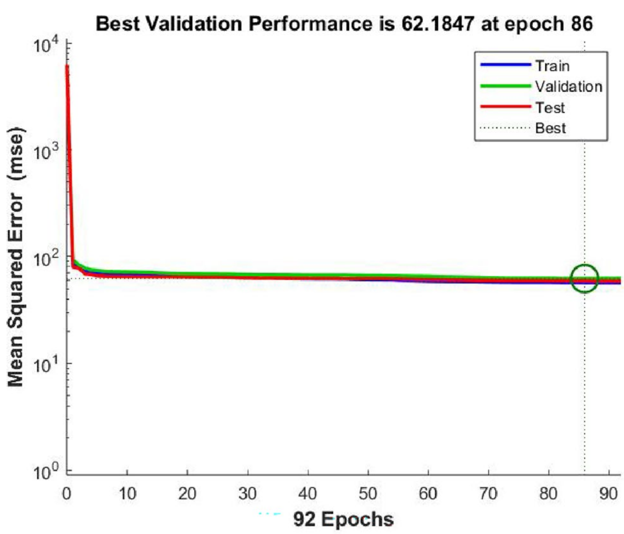

Fig. 40 Generalization error of Optimized Back-propagation ANN

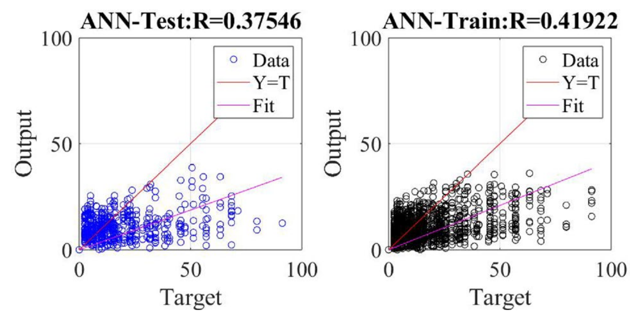

Fig. 41 Regression coefficients of ANN, in terms of rebar cross-section area (cm^2)

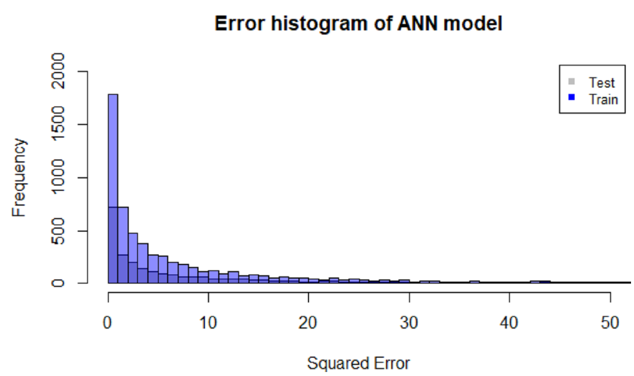

Fig. 42 Error histogram for ANN

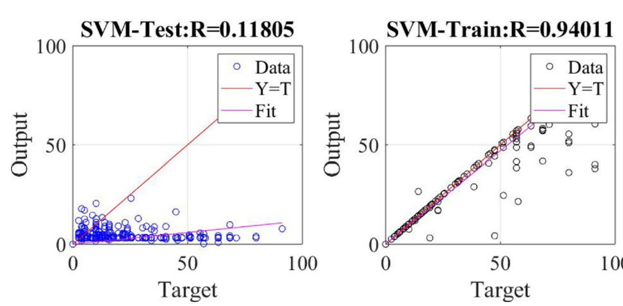

Fig. 43 Regression coefficient, in terms of rebar cross-section area (cm^2), for optimized non-linear SVM model

- Maximum number of epochs equal to 1000.
- Maximum validation failures equal to 3.
- Test ratio and validation ratio equal to 0.15.
- Train goal equal to 1×10^{-9}.

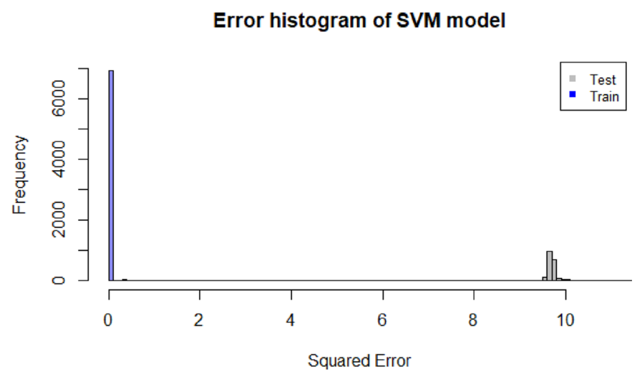

Fig. 44 Error histogram for non-linear SVM model

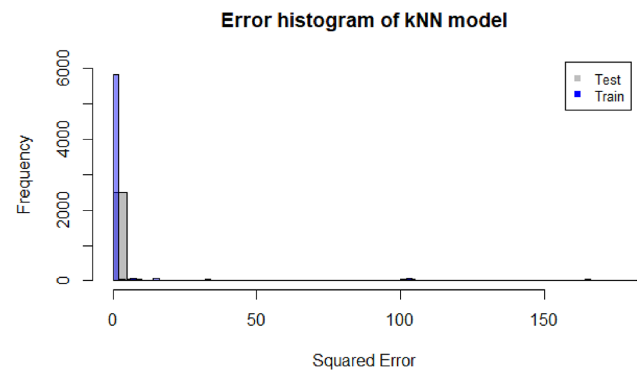

Fig. 47 Error histogram for optimized *k*-NN with $k = 8$ and *city-block* distance metric

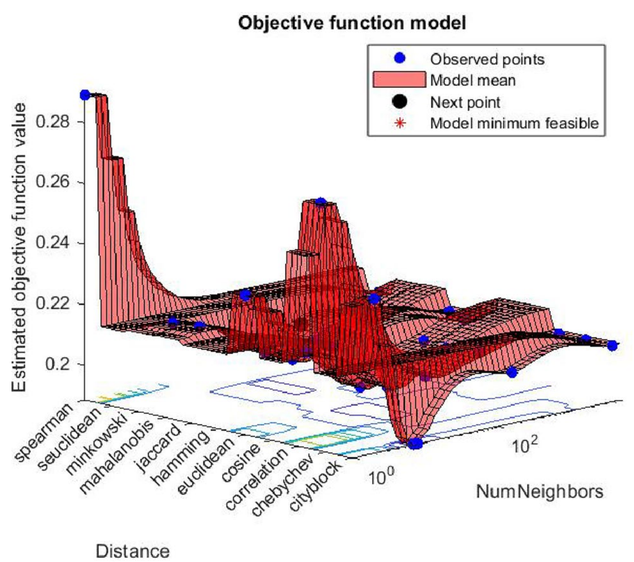

Fig. 45 Model search for hyper-parameter optimization of *k*-NN model

The MSE performance in function of epochs is shown next (Fig. 40):

The regression coefficient results and error histograms are shown below (Fig. 41, 42), respectively:

C.1.4 Support vector machines

For SVM, Sequential minimal optimization was used as solver, for a Gaussian Kernel. After Bayesian Optimization, the following optimum hyper-parameters were found:

- Box constraint equal to 70.22.
- Kernel scale equal to 0.0.5709.
- Epsilon equal to 0.000838.

The regression coefficients and error histograms are shown below (Fig. 43, 44), respectively:

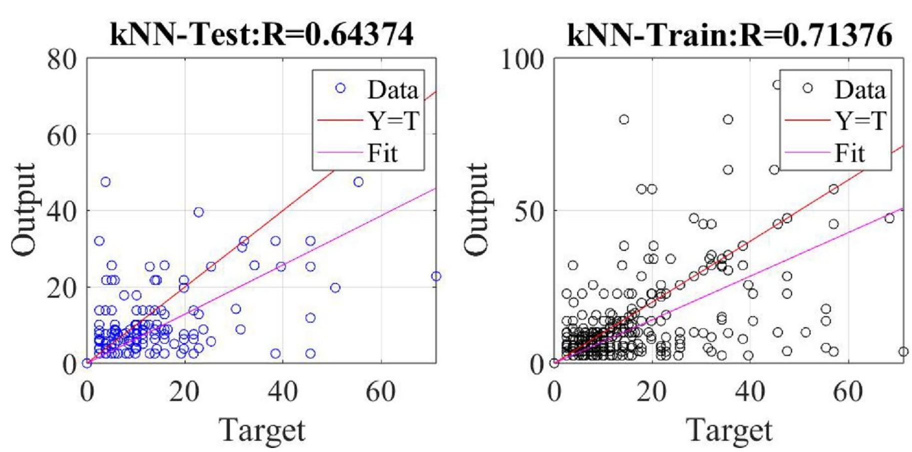

Fig. 46 Regression coefficient, in terms of rebar cross-section area (cm^2), for optimized *k*-NN with $k = 8$ and *city-block* distance metric

Fig. 48 (Left panel) summary of MSE performance of pure ML models for enhancement. (Right panel) summary of Regression coefficients of pure ML models for enhancement

C.1.5 *k*-Nearest neighbor

For *k*-NN, after hyper-parameter optimization (Fig. 45), $k = 8$ and the *city-block* metric were set to train the model. The corresponding regression coefficients and error histogram, with the optimized model, are shown in (Fig. 46, 47), respectively.

C.2 Summary of performance of pure ML models

Based on the optimized ML models just presented, with a data size of 10,000 samples, with a 7/3 training/testing proportion, the performance of each model, in terms of MSE and regression coefficients is summarized in the following bar plots (Fig. 48):

As it can be observed, SVM has the worst performance when applying it to new data, but the best for training data. That is, when using the SVM for this problem, it tends to underfit for new predictions, in a great deal. This underfitting can be appreciated in their corresponding regression plots, presenting a great bias, which in turn, can be related to the high obtained MSE values. Based on these results, it would be expected for the ML-Enhanced MA to perform in a similar way, especially in terms of these same metrics.

Table 7 Algorithmic parameters for the ML-Enhanced meta-heuristic optimization algorithms with the PSO and the GA

PSO	GA
$\alpha = 1$	$N_{\text{generations}} = 25$
$c_1 = 2, c_2 = 2$	$P_{\text{mutation}} = 0.06$
$\Delta t = 0.5$	$\text{selection}_{\text{tournament}} = 0.8$
$\text{weight}_{\text{inertia}} = 1.3$	$N_{\text{population}} = 30$
$\beta = 0.99$	$\text{size}_{\text{tournament}} = 2$
$N_{\text{particles}} = 30$	$P_{\text{cross-over}} = 0.65$
$\max_{\text{iterations}} = 25$	$N_{\text{genes}} = 80$
$N_{\text{variables}} = 4$	$N_{\text{variables}} = 4$
$\text{Range}_{\text{variables}} = [1, \text{Ndiam}]$	$\text{Range}_{\text{variables}} = [1, \text{Ndiam}]$

Appendix 4: Generalized performance of ML-Enhanced optimization algorithms

To effectively assess the general algorithmic efficiency of ML-Enhanced Meta-heuristics for the optimal design of rebars in a reasonable amount of time, the problem should be formulated as SO. For such case, the objective function corresponding to the rebar cross-section area is to be minimized. This way, after the optimization process is terminated, a direct comparison of the optimal values found with ML-Enhanced Meta-heuristic can be made with those real optimal ones from the test data.

In contrast to MO optimization problems, for SO a solution $x_1 \in S$ is better than another solution $x_2 \in S$ if $f(x_1) < f(x_2)$, so that its formulation can be expressed as in (23). In such formulation, $f(x)$ is the objective function, x is the compound of design variables (which for this formulated problem of rebar design $k = 4$, namely the rebar diameters at each of the four cross-section's edges, in a discrete form). Thus, x_j^{L} and x_j^{U} would represent the upper and lower range limits of each variables x_j, under design i constraints $g_i(x)$.

$$\begin{aligned} &\min[F(x) = f(x)] \\ &\text{S.T.:}\, x_j^{\mathrm{L}} \leq x_j \leq x_j^{\mathrm{U}}, \quad j = 1, 2, \ldots, k. \\ &\text{under: } g_i(x) \leq y_i, \quad i = 1, 2, \ldots, q. \end{aligned} \tag{23}$$

The same design constraints stated for MO optimization were considered for SO to showcase. The objective function was considered as the cross-section rebar area to be minimized. Two meta-heuristic optimization algorithms were used, the PSO and GA. Each of them were enhanced with the same ML techniques as for MO optimization. Scenario 1 of commercial rebar availability described in Table 5, from "Appendix 2", corresponding to 7 available rebar diameters was considered ($x_j^{\mathrm{L}} = 1, x_j^{\mathrm{U}} = 7$). A detailed description of each ML-Enhanced SO algorithm is presented in "Appendix 4", in pseudo-code.

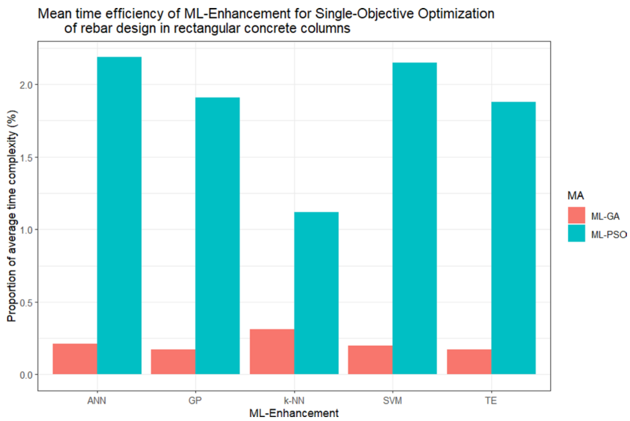

Fig. 49 Mean time efficiency of each ML-Enhanced SO optimization algorithm for rebar design

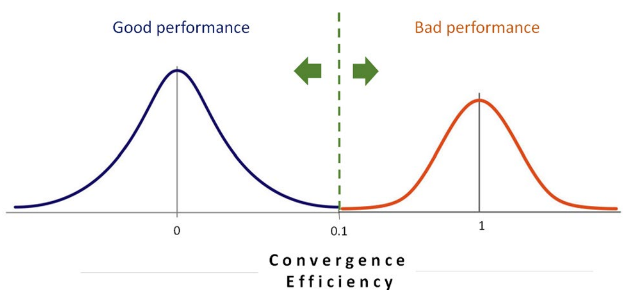

Fig. 50 Definition of good/bad performance of an ML-Enhanced MA to measure its Accuracy for rebar optimization design

D.1 Time efficiency of ML-Enhanced optimization algorithms for the shown-case data size $N = 10{,}000$

One of the advantages of Combinatorial Optimization (CO) is that the time efficiency of any SO optimization algorithm for the design of rebar in rectangular concrete columns can be measured. This is achieved by the characterization of rebar design complexity from which the average worst case number of potential design evaluations is considered as reference.

The complexity characterization of scenario 1 of commercial rebar availability corresponds to Fig. 33 (Top-Left) where the average worst case number of potential designs can be measured as (24), in function of the columns' cross-section width dimension b. To measure the accuracy of each ML-Enhanced algorithm the relative error formula was used as in (25), where N_{eval} represents the total number of evaluations needed for each ML-Enhanced algorithm to reach an optimum solution. In this sense, the algorithmic parameters for the PSO and the GA were set as shown in Table 7 so that both would have the same number of max possible evaluations, for better comparison:

$$N_{d_1} = e^{8.69706+0.037836 \cdot b}, \quad , \tag{24}$$

$$N_{\text{eval}} = 1 - \frac{N_{d_1} - N_{\text{eval}}}{N_{d_1}}. \quad . \tag{25}$$

For the data size of 10,000 samples considered for the shown-case column models, a fraction of 70% was taken for training and 30% for testing. The efficiency obtained is resumed in Fig. 49 in terms of mean efficiency values, for all ML-Enhancement. It can be observed that TE had the best performance when used for the GA and the second best performance when used for the PSO. In summary, a reduction of the search space could be reduced to approximately proportions no more than 2.5% with the PSO and 0.4% with the GA.

D.2 Convergence efficiency of ML-Enhanced SO optimization algorithms for the shown-case data size N=10,000

To assess the convergence efficiency of the ML-Enhanced algorithms with this data size used for showcase, the accuracy (portion of good/bad optimal designs) and regression

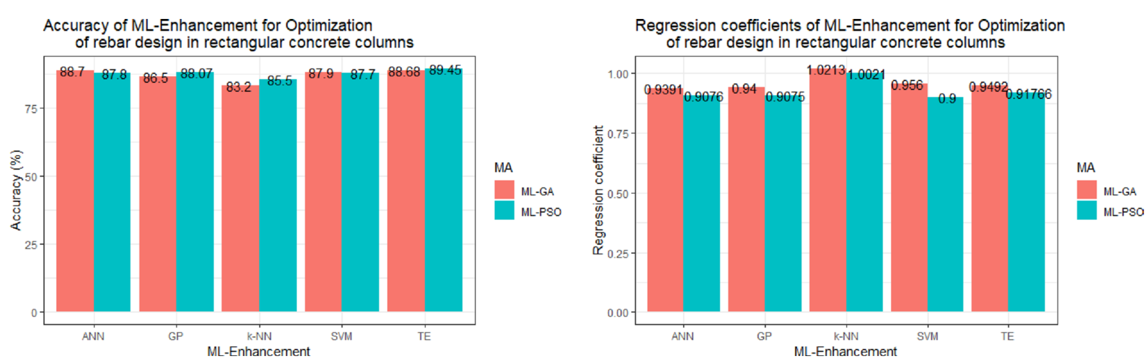

Fig. 51 (Left panel) Accuracy of convergence of each ML-Enhanced meta-heuristic optimization algorithm for a testing data size of 3000 out of a total of $N = 10,000$ samples. (Right panel) Corresponding test regression coefficients

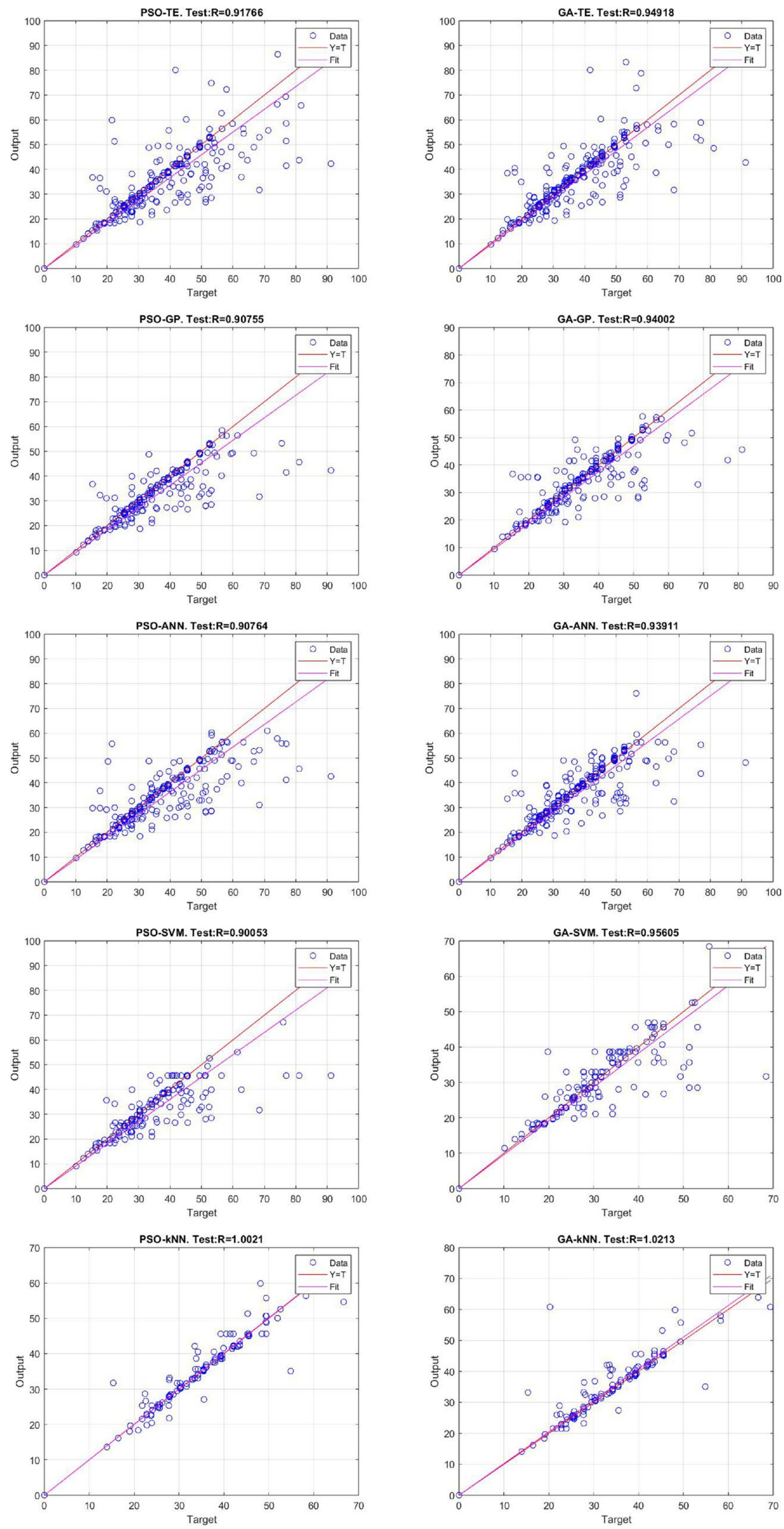

Fig. 52 Regression test coefficients, in terms of rebar cross-section area (cm^2), for the ML-Enhanced Meta-heuristics for the shown-case data size $N = 10{,}000$. (Left) ML-PSO. (Right) ML-GA

coefficient are used. The accuracy is based on the relative error criteria (26), as shown in Fig. 50, where A_{CO} is the optimal rebar cross-section area obtained with CO and A_{ML} is the optimal rebar area obtained with the ML-Enhanced algorithm.

$$\mathrm{MRE} = \frac{A_{\mathrm{ML}} - A_{\mathrm{CO}}}{A_{\mathrm{CO}}} \quad . \tag{26}$$

Under this criteria, the performance of the ML-Enhanced meta-heuristics for the data size of 10000 samples generated for the shown-case column models from Figs. 14 and 17 is shown next. The portion of 70%/30% training/testing was considered. As it can be observed in Fig. 51 (Left), Tree Ensembles, Gaussian Process, and ANN demonstrated to have the best accuracy. The regression coefficients are shown next in Fig. 52, with their corresponding summary of results in Fig. 51 (Right). It can be observed that, in terms of regression coefficients, there is a great correlation in reference to the regression coefficients obtained for the pure ML models, that is, having the k-NN the highest performance as before and the SVM the lowest. However, the increase between the regression coefficient values of each pure ML model and its corresponding ML–MA enhancement is more than evident. The highest correlation coefficient that the *k*-NN provides for MA enhancement does not imply that it performs better than the others, in general. This fact can be observed when looking at the accuracy results. Even though *k*-NN has the best performance, its accuracy is the lowest, which indicates a high variance, and therefore, overfitting for new data, which can be also observed in the high obtained MSE of their corresponding pure ML version in Fig. 48.

Another important observation from the regression plots is the high bias that the SVM, ANN, TE, and GP-enhanced MA have for higher optimum reinforcement cross-section areas. That is, the larger the cross-section dimensions and/or loads for a column, the higher the probability to obtain high errors of prediction.

D.3 Generalization of performance of ML-Enhanced Meta-heuristics

In this section, for generalized validation of performance of the ML-Enhanced optimization algorithms, in addition to the accuracy, regression coefficient, mean relative error (MRE), and mean squared error (MSE) as metrics for performance assessment, the R^2 score is also considered. The results can be visualized in Fig. 53, as the data size increases, for both meta-heuristics. In summary, it can be observed that k-NN performed the worst, for all metrics and for both MA. The rest of ML enhancements demonstrated to be very competitive between each other, for all cases, although TE, ANN, and GP demonstrated better performance for small data sizes of less than 10,000. In general, the use of the PSO demonstrates to have better performance than the GA, for any case. To carry out these regularization experiments, a different ML model was trained for each data size, where for each ML model, three optimization processes where executed and averaged. The purpose of this experimentation scheme was to get rid of the stochastic property of the ML-Enhanced algorithms due to the meta-heuristics, as much as possible, and have more reliable estimates of the performance.

As it can be observed from these results, levels of accuracy above 85% were demonstrated for both MAs for data sizes as small as 1000 samples. The R^2 score was considered as the metric of reference to establish a termination criteria of data size sufficiency for training (see third row from the previous plots). By considering a criteria of $\Delta(R^2) \leq 0.5\%$ *for every additional 1000 samples*, the following maximum data sizes of Table 8 are obtained:

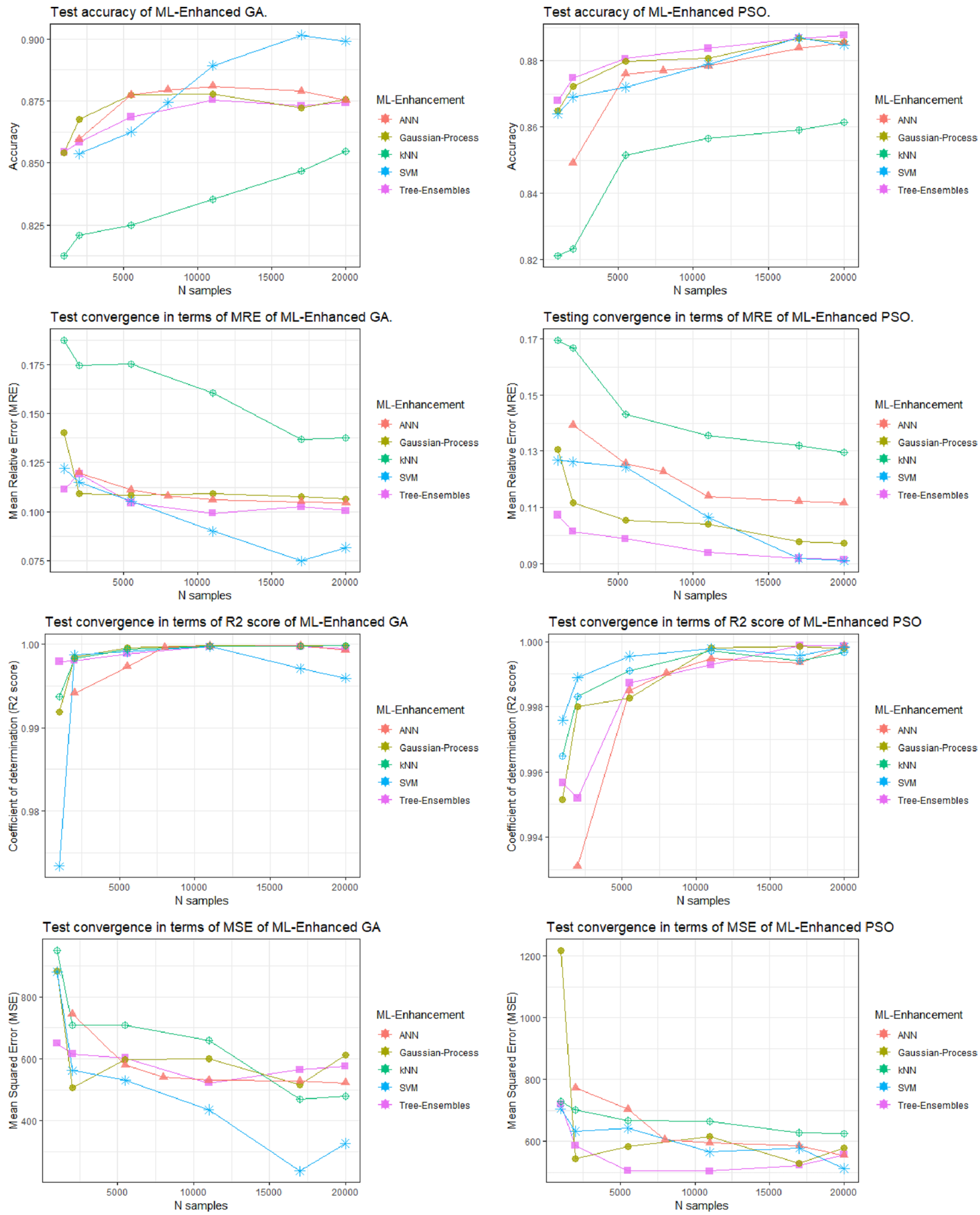

Fig. 53 Test performance of ML-Enhanced algorithms as the data size increases. Left: ML-Enhanced GA. Right: ML-Enhanced PSO

Table 8 Minimum data size (number of samples) required for training to reach the criteria of $\Delta(R^2) \leq 0.5\%$ *for every additional 1000 samples*

ML/MA	GA	PSO
TE	11, 000 Samples	17,000 Samples
GP	11,000 Samples	11, 000 Samples
ANN	11, 000 Samples	11,000 Samples
SVM	8 000 Samples	11,000 Samples
k-NN	17, 000 Samples	11,000 Samples

Appendix 5: SO optimization ML-Enhanced algorithms in pseudo-code

Algorithm 1: ML-Enhanced Genetic Algorithm for SO optimization of rebar design (ML-GA)

A. Build ML model
A.1 Import data
A.2 According to the given values: cross-section dimensions (b, h) for the column, compressive strength of concrete used (f'_c), axial load resistance percentage $ppoc$ and biaxial load eccentricities e_x, e_y, perform ML regression/classification to obtain an optimum quantity of reinforcement area for each cross-section's edge
B. ML-Enhanced GA for rebar design optimization
B.1 Initialize population randomly through the creation of N chromosomes (strings of binary digits) that represent each individual of the population:
$x_i = [diam_{index-1}, diam_{index-2}, diam_{index-3}, diam_{index-4}]$, where $diam_{index-j}$ takes a discrete integer value between $[1, 7]$ corresponding the index of each rebar diameter in the initial given database of commercial available rebars
B.2 Generate the next generation
B.2.1 Evaluate individuals of the current generation with the objective function with the variable values obtained through the de-codification of chromosomes so that a fitness value is determined for each individual.
B.2.2 Select a pair of individuals of the current evaluated generation. Those with the highest fitness values should have more probability of being selected
B.2.3 Generate a new chromosome with the pair of individuals selected through crossover
B.2.4 Mutate the chromosome
B.2.5 Repeat steps B.2.1 to B.2.4 until N new individuals are generated for replacement
B.3 Return to step B.2 until a convergence or termination criteria is reached

Algorithm 2: ML-Enhanced Particle Swarm Optimization algorithm for SO optimization of rebar design(ML-PSO)

A. Build ML model
A.1 Import data
A.2 According to the given values: cross-section dimensions (b, h) for the column, compressive strength of concrete used (f'_c), axial load resistance percentage *ppoc* and biaxial load eccentricities e_x, e_y, perform ML regression/classification to obtain an optimum quantity of reinforcement area for each cross-section's edge
B. ML-Enhanced PSO for rebar design optimization
B.1 Initialize positions and velocities of each particle p_i
$x_{ij} = 1 + rand \cdot (7-1), i = 1, ..., Nparticles, j = 1, ...4$
$v_{ij} = \frac{\alpha}{\Delta t}(-\frac{7-1}{2} + rand \cdot (7-1)), i = 1, ..., Nparticles, j = 1, ...4$
B.2 Evaluate each particle in the swarm through the objective function $f(x_i), i = 1, ..., Nparticles$.
B.3 Update the best position during the evaluation of each particle (if a) is complied)) and the best global position (if b) is complied))
a.) if $f(x_i) < f(x_i^{pb})$ then $x_i^{pb} \cdots x_i$
b.) if $f(x_i) < f(x^{sb})$ then $x^{sb} \cdots x_i$
B.4 Update velocities and positions:
$v_{ij} \cdots v_{ij} + c_1 q(\frac{x_{ij}^{pb} - x_{ij}}{\Delta t}) + c_2 r(\frac{x_j^{sb} - x_{ij}}{\Delta t}), i = 1, ..., N, j = 1, ..., n$
Restrict velocities, such that $|v_{ij}| < v_{max}$
$x_{ij} \cdots x_{ij} + v_{ij}\Delta t, i = 1, ..., N, j = 1, ..., n$
B.5 Return to step B.2, unless the termination criteria is reached

Appendix 6: Potentials of savings of material and construction cost with asymmetrical optimal rebar

To fully appreciate the advantages of designing optimal asymmetrical rebar in rectangular concrete columns when subject to asymmetrical bending compression loads it is first necessary to establish a metric to measure how symmetrical or asymmetrical a given pair of bending loads is. For this purpose, a Degree of Load Symmetry (DLS) concept has been developed, in which three main cases were identified according to the load eccentricities of any given pair of load combinations, as shown next in Fig. 54. The symmetry/asymmetry is computed by considering only the bending loads and their components. A max value of 1 represents a purely symmetrical set of load conditions, that is, when the component of each bending load are mirrored with one another with respect to each of the cross-section axis. On the other hand, a min value of 0 would represent a pure asymmetrical set of loads—most likely when the components of both bending loads have the same direction.

Once a measure of Load Symmetry has been stated, then the relationship and tendency of rebar volume savings and/or construction cost savings with respect to such DLS using asymmetrical optimal rebar designs could be assessed. For this purpose, 120 random columns with a given set of pair of load conditions were generated and optimally designed for five different levels of Constructability (CFA). The results are depicted in Fig. 55. Such experimentations were executed only for the Rebar Prototypes (Assem-1rebar) described in "Appendix 2", corresponding to designs in individual rebars. The unit construction costs for any rebar design were computed based on the unit cost card shown in Table 2 parameterized with respect of the CFA. The weight factors required for the computation of the CFA for any rebar design were taken as $W_{\mathrm{unb}} = 1$ and $W_{\mathrm{ND}} = 2$.

A clear tendency can be observed in Fig. 55 (Left) for the rebar volume savings to increase as the DLS decreases,

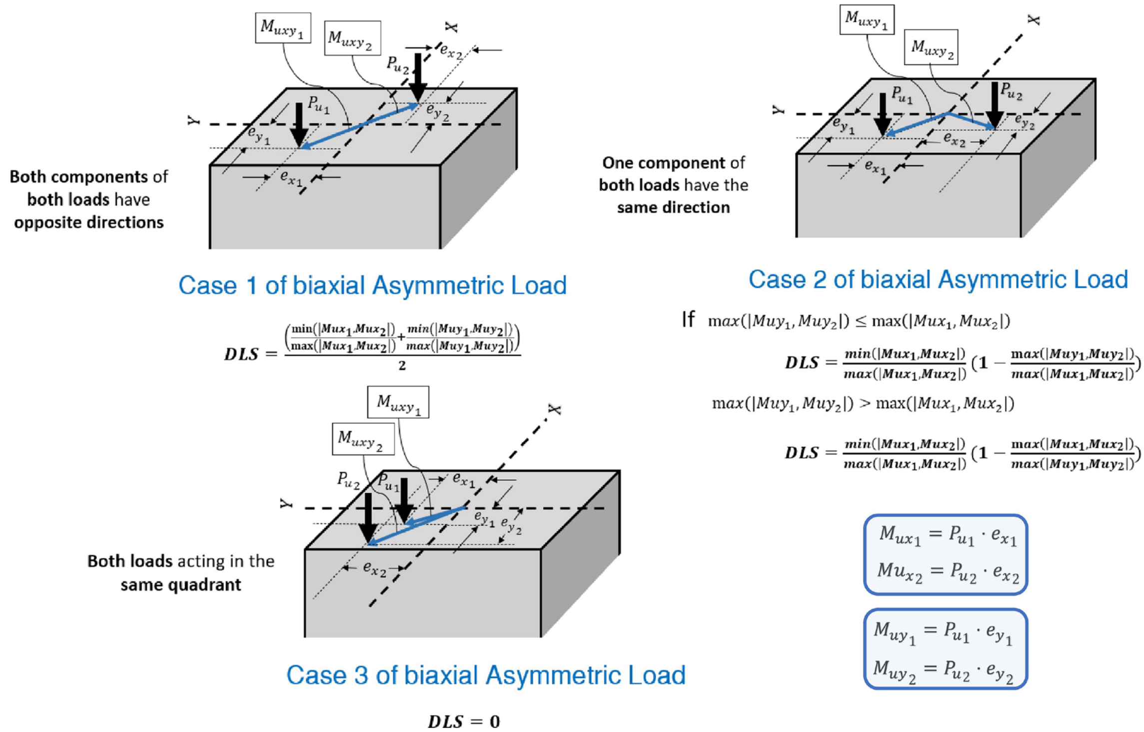

Fig. 54 Measurement of the Degree of Load Symmetry. Three main cases are considered. Case 1: both components of both loads have opposite directions, Case 2: one component of both loads have the same direction, and Case 3: both components of both loads have the same direction

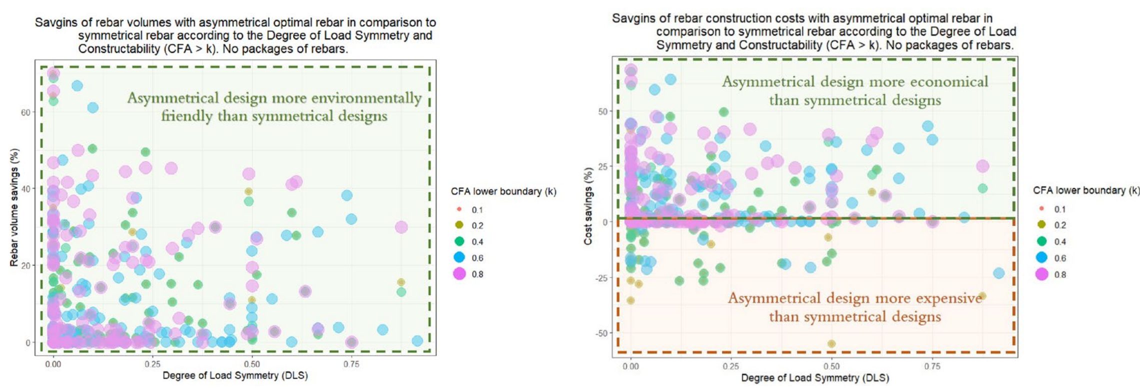

Fig. 55 Tendency of rebar volume savings (left panel) and construction costs (right panel) generated with optimal asymmetrical rebar designs in columns with respect to the Degree of Symmetry of the applied loads DLS. The higher the DLS, the more symmetrical the loads with respect to both axis of the cross-section. Five different levels of constructability are depicted

that is, for highly asymmetrical loads. A similar pattern can be observed for the construction cost savings in Fig. 55 (Right), although for the latter, a considerably large number of designs tuned out to be more expensive (negative saving values). However, such negative savings are observed to be mitigated for moderate levels of constructability (CFA lower boundary values higher than 0.6). Nevertheless, the positive potential savings, both of rebar volumes and construction costs, reached considerably higher values of more than 50%, even for higher constructability levels (Fig. 56).

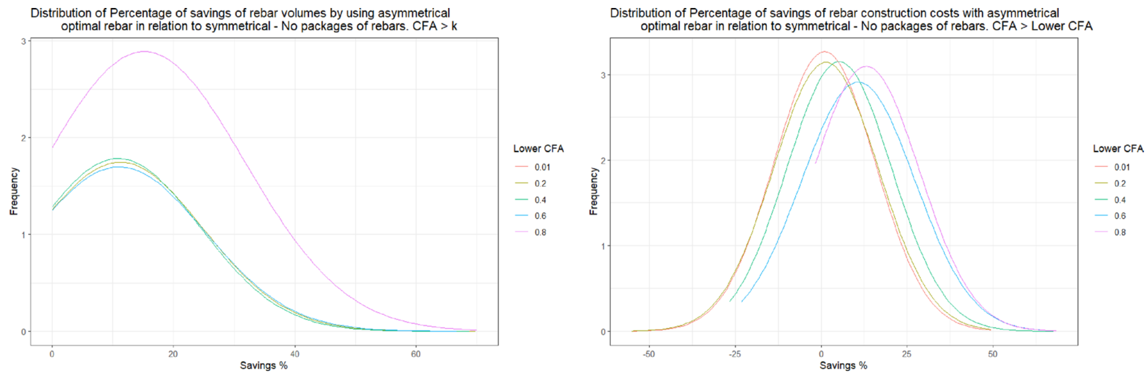

Fig. 56 Distribution of savings of rebar volumes (Left panel) and construction costs (Right panel) for different levels of desired constructability, using asymmetrical optimal rebar, in comparison with symmetrical conventional designs

Appendix 7: Breakdown of the Buildability Score model

In the next figure, a 3D representation of the BS model for nine different weight factor ratios is presented, for better appreciation of the BS function, when asymmetrical rebar designs, are in general not desired. In this nine cases, both weight factors are larger or equal than 1, penalizing any form of asymmetrical distribution of the rebars (both asymmetry of distribution of number of rebars and asymmetry of distribution of rebar diameter sizes) in their cost (Fig. 57).

As it can be observed, the higher the values of the weight factors the more concave the surface becomes, indicating the penalization feature as either of the variable values change. For small values of the weight factors, the surface tends to become flat.

It is to note that for those extreme cases (corners of the surface where $\mathrm{ND} = 4, \mathrm{UNB} = 1$ and $\mathrm{ND} = 1, \mathrm{UNB} \approx 0$) to have the same value, then, the condition (27) must be satisfied:

$$\begin{aligned} &1^{W_{\mathrm{UNB}}} + \frac{1}{4^{W_{\mathrm{ND}}}} = \min(\mathrm{UNB})^{W_{\mathrm{UNB}}} + \frac{1}{1^{W_{\mathrm{ND}}}} \\ &-W_{\mathrm{ND}} \cdot \ln(4) = W_{\mathrm{UNB}} \cdot \ln(\min(\mathrm{UNB})). \end{aligned} \tag{27}$$

In this sense, when the Non-Uniformity of Number of rebars (small values of UNB) is preferred, which would be usually the case instead of the Variability of Number of rebar Diameters (high values of ND), then the ratio $W_{\mathrm{UNB}}/W_{\mathrm{ND}}$ would be defined as follows (28:

$$\frac{W_{\mathrm{UNB}}}{W_{\mathrm{ND}}} \leq -\frac{\log(4)}{\log(\min(\mathrm{UNB}))}. \tag{28}$$

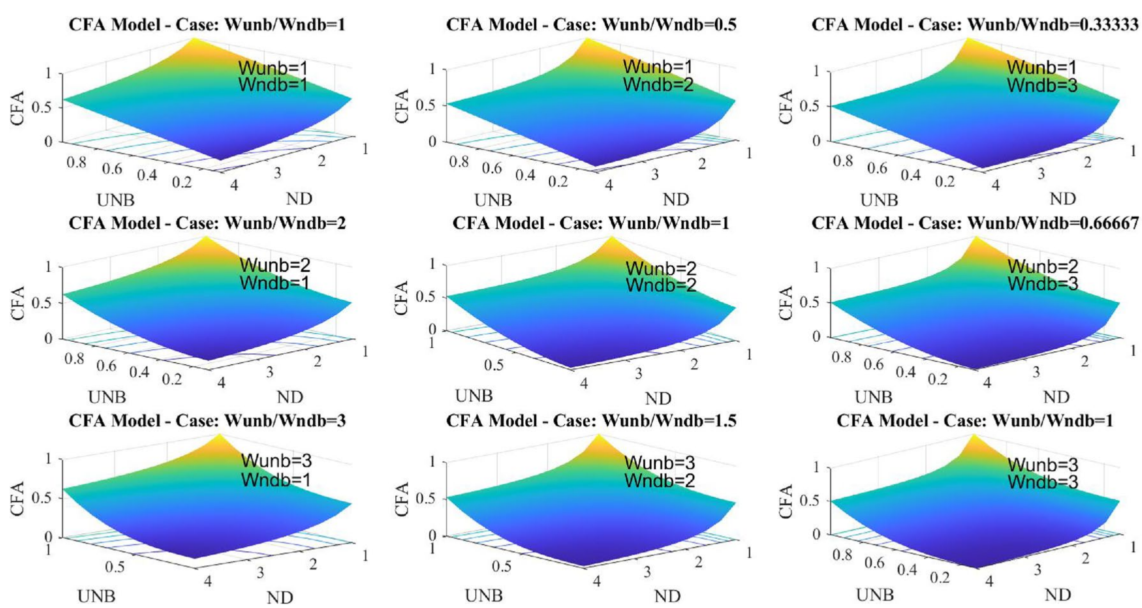

Fig. 57 3D graphic depiction of the normalized BS parametric model (CFA) according to the *Uniformity of Number of Rebars* and *Number of Rebar Diameters*, for 9 different weight ratios, with weight factor values larger or equal than 1

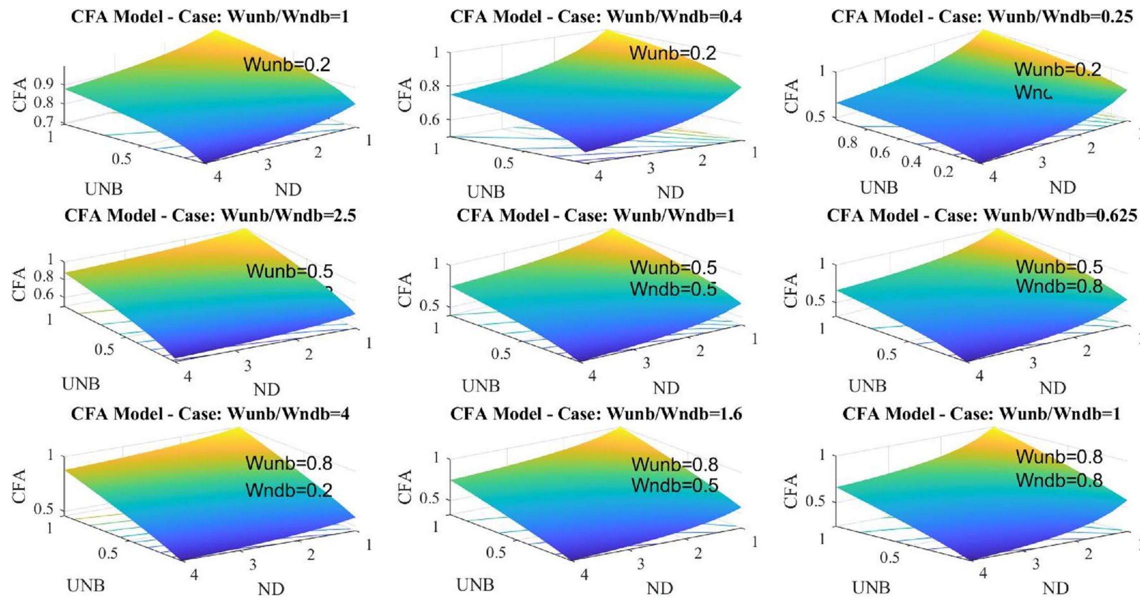

Fig. 58 3D graphic depiction of the normalized BS parametric model (CFA) according to the *Uniformity of Number of Rebars* and *Number of Rebar Diameters*, for 9 different weight ratios, with weight factor values less than 1

In general, a reasonable min value of the Uniformity of Number of Rebars (UNB) could be considered as min(UNB) = 0.1, as it was considered for this research, and for which

$$-\frac{\log(4)}{\log(\min(\mathrm{UNB}))} \approx 0.6. \tag{29}$$

Meaning that, in order for the BS model to consider a preference on the uniformity of number of rebars, the weight factor $W_{\mathrm{UNB}}/W_{\mathrm{ND}}$ is recommended to be less or equal than 0.6. Otherwise, the BS model would penalize more those designs with variability of numbers of rebars at each cross-section boundary and penalize less the designs that have a high variability of rebar diameters (which is not usually the preferred case, given that diameter sizes of rebars are sold by tons). The individual values of each weight factor, however, would depend on how flat (linear) or curved (non-linear) is the surface desired to be.

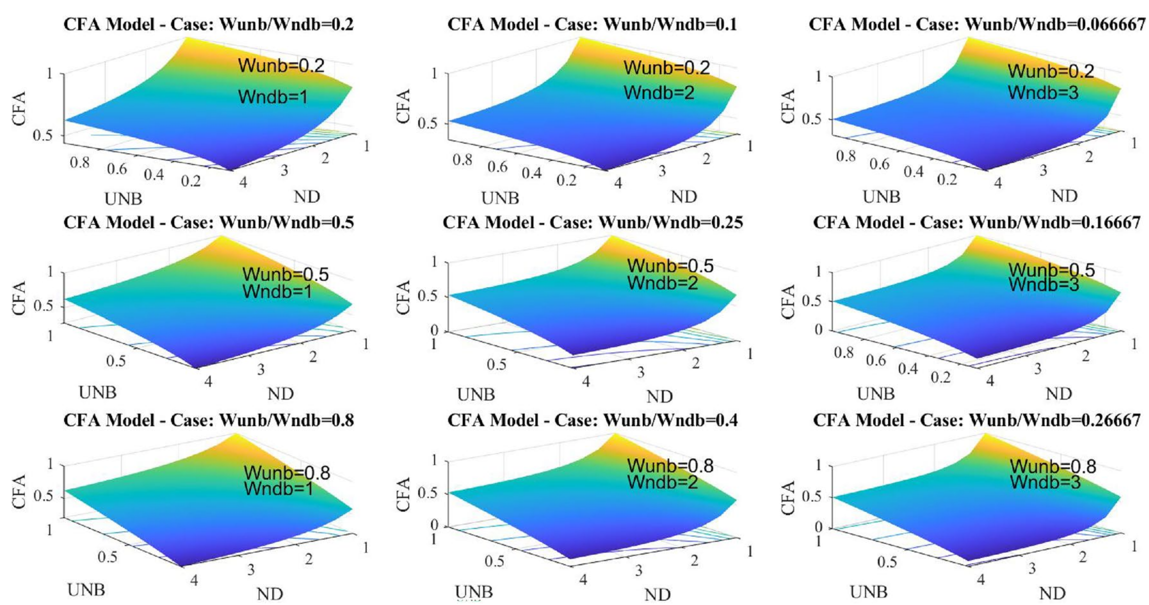

Fig. 59 3D graphic depiction of the normalized BS parametric model (CFA) according to the *Uniformity of Number of Rebars* and *Number of Rebar Diameters*, for 9 different weight ratios, with $W_{\mathrm{UNB}} < 1$ and $W_{\mathrm{ND}} > 1$

Figure 58 depicts the behavior of the BS model for both weight factors less than 1 (small penalization for the variability of number of diameters and a preference for the asymmetry of number of rebars). Note that, regardless of the weight factor individual values, when the ratio is less than 0.6, the constructability turns out to be slightly higher when ND → 1.

Finally, the next figure depicts the behavior of the BS function for the standard case, when the asymmetry of number of diameter sizes is penalized in a great deal $W_{\mathrm{ND}} > 1$, being the asymmetry of number of rebars the preferred case W_{UNB}, when searching for asymmetrical rebar designs. In contrast the previous second case, the constructability of the rebar designs when ND → 1 and when $W_{\mathrm{UNB}}/W_{\mathrm{ND}} \leq 0.6$ tends to exponentially increase (Fig. 59).

Appendix 8: Abbreviations and notations

See Tables 9 and 10.

Table 9 List of abbreviations

Abbreviations	
AEC	Architecture, Engineering and Construction
ANN	Artificial Neural Networks
BDAS	Buildability Design Appraisal System
BS	Buildability Score
CAL-software	Computer-Aided Learning software
CFA	Constructability Factor of rebar Assembly
CIRIA	Construction Research and Information Association
CO	Combinatorial Optimization
DfMA	Design of Manufacturing and Assembly
DLS	Degree of Load Symmetry
GA	Genetic Algorithm
GNN	Graph Neural Networks
GP	Gaussian Process
k-NN	*k*-Nearest Neighbor
LHS	Latin Hypercube Sampling
MA	Meta-heuristic algorithms
MIGD	Mean-Inverted Generational Distance
ML	Machine Learning
MO	Multi-Objective
MRE	Mean Relative Error
NSGA-II	Non-Sorting Genetic Algorithm II
PBD	Performance-Based Design
PF	Pareto Front
PSO	Particle Swarm Optimization
TE	Tree Ensembles
RC	Reinforced Concrete
rebar	Reinforcing bar
RP	Rebar Prototype
SO	Single Objective
SVM	Support Vector Machines

Table 10 List of notations of variables

Notations for variables.	
$A_{\mathrm{o}}^{\mathrm{LS}}$	Optimum reinforcement area determined with combinatorial algorithms based on Linear Search based
$A_{\mathrm{o}}^{\mathrm{ML}}$	Optimum reinforcement area obtained by a ML-Enhanced algorithm
A_s	Cross-section reinforcement area
b	Cross-section width dimension
c	Neutral axis depth of a column cross-section
cover	Concrete cover
$\mathrm{db}_1, \mathrm{db}_2, \mathrm{db}_3, \mathrm{db}_4$	Diameter of rebars at the top, bottom, left, and right edge of a rectangular cross-section
db	Diameter of bar
d	Effective depth of a column cross-section
e_x	Load eccentricity along the X axis
e_y	Load eccentricity along the Y axis
Eff	Structural resistance efficiency
f_c'	Compressive strength of concrete
Fev	Scale factor of Number of design evaluations for the estimation of rebar complexity
$\mathrm{Ef}_{\mathrm{conv}}$	Convergence efficiency
h	Cross-section height dimension
Nar	Number of available commercial rebars
$\mathrm{nb}_1, \mathrm{nb}_2, \mathrm{nb}_3, \mathrm{nb}_4$	Number of rebars at the top, bottom, left and right edge of a rectangular cross-section
$\mathrm{Nd}^{\mathrm{LS}}$	Average Number of design evaluations needed through Linear Search
$\mathrm{Nd}^{\mathrm{ML}}$	Number of design evaluations performed by a ML-Enhanced algorithm
ND	Number of Diameters placed over a rectangular cross-section
$\mathrm{ND}_{\mathrm{com}}$	Number of commercial rebar Diameters available in a market
$N_{\text{ev-max}}^{\text{1pack-assem}}$	Theoretical combinatorial number of potential design evaluations of rebar designs in individual rebars
$N_{\text{ev}}^{\text{1pack-assem}}$	Numerical estimation of number of potential design evaluations of rebar designs in individual rebars
Ppoc	Percentage of axial resistant force in compression
$\mathrm{sep}_{\mathrm{min}}$	Minimum rebar separation set by code specifications
UNB	Uniformity of Number of Rebars
W_{UNB}	Weight factor for the variable UNB
W_{ND}	Weight factor for the variable ND
ϵ_t	Max steel strain in tension
ϕ	Resistance reduction factor

Acknowledgements This research was possible thanks to the Hong Kong University of Science and Technology (HKUST) for the partial financial support provided through a Graduate Scholarship. Thanks to my PhD Supervisor Dr. Jize Zhang for his suggestions while training the ML models. Thanks to Dr. Luo Bo for his support in the Multi-objective optimization part to analyze the convergence of the algorithms.

Author contributions L.F. Verduzco contributed to Conceptualization, Methodology, Software, Formal analysis, Investigation, Data curation, Writing and original draft preparation, and Writing—review and editing.

Funding Open access funding provided by Hong Kong University of Science and Technology. This research was partially supported financially by the Hong Kong University of Science and Technology (HKUST) as a Graduate Scholarship.

Data availability The data that supports the findings of this study are available on request from the corresponding author.

Code availability For the computation of 3D interaction surfaces for rectangular columns to determine their resistance the Open Source software CALRECOD was used: https://github.com/calrecod/CALRECOD. Additional code for optimization and Machine Learning models remains private.

Materials availability The materials used for this research are not publicly available.

Conflict of interest The authors have no competing interests to declare that are relevant to the content of this article.

Replication of results

(1) Automate the efficiency analysis process for concrete columns, according to the applicable design hypothesis, following a linear mechanical behavior and linear distribution of stresses over a cross-section. For this purpose, the computation of interaction surfaces as shown in Fig. 6 is suggested. At this stage, make sure to implement all the applicable design restrictions as in (3) to (9). Various Open Source software could be used for this purpose, in MATLAB or Python, such as CALRECOD https://github.com/calrecod/CALRECOD.

(2) Train the ML model using the data architecture as shown in Fig. 10 and its corresponding variables' range values, as shown in Fig. 13. For this purpose, deploy combinatorial optimization to find an optimal rebar design for each data sample (column) for efficiency analysis under SO. Follow the formulation established in "Appendix 1" and the criteria established in "Appendix 2" with the corresponding design restrictions. Choose the scenario 1 of commercial rebar availability from Table 5. For MO optimization, compute the two-staged NSGA-II from Fig. 12 and extract the optimum design with the lowest rebar cross-section area, from the PF. Once the optimum rebar design is determined for each column sample, use the rebar cross-sectional area quantities at each of the four column's cross-section's boundaries to feed the training data. These rebar cross-sectional areas are the values to be predicted by the ML model.

(3) Compute the constructability of rebar designs according to the BS model here proposed in (2). Choose the weight factors as appropriate, according to the results of this research.

(4) Compute the unit cost of rebar designs in rectangular concrete columns according to the unit cost card shown in Table 2.

(5) Implement the NSGA-II so that the optimization variables are set merely as the rebar diameter sizes, for any given column to be designed. Set the objective functions as shown in (10). Any public repository of this algorithm can be used, such as https://www.mathworks.com/matlabcentral/fileexchange/52869-non-dominated-sorting-genetic-algorithm-ii-nsga-ii. Adjust the algorithmic parameters as appropriate according to the results of this research.

(6) For each combination of rebar diameter sizes use, the trained ML model by passing it the corresponding features of the column to be designed (cross-section dimensions b, h, compressive strength of concrete f'_c, axial compression load P_u, biaxial load eccentricities e_x, e_y). The ML model's prediction of optimum rebar cross-sectional area, is then, used to determine an optimum combination of number of rebar diameters at each of the four column's cross-section boundaries, according to the sizes of rebar diameters.

References

ACI (2019) ACI318, building requirements for structural concrete and commentary ACI 318–19. ACI, Farmington Hills

Adams S (1989) Practical buildability. Butterworths/CIRIA, Sevenoaks

Afshari H, Hare W, Tesfamariam S (2019) Constrained multi-objective optimization algorithms: review and comparison with application in reinforced concrete structures. Appl Soft Comput J 83:105631

Afzal M, Maqsood S, Yousaf S (2017) Performance evaluation of cost saving towards sustainability in traditional construction using prefabrication techniques. Int J Res Eng Sci 5:73–79

Afzal M, Liu Y, Cheng JCP, Gan VJL (2020) Reinforced concrete structural design optimization: a critical review. J Clean Prod 260:120623

Ahmadkhanlou F, Adeli H (2005) Optimum cost design of reinforced concrete slabs using neural dynamics model. Eng Appl Artif Intell 18:65–72

Alanani M, Brown T, Elshaer A (2024) Multiobjective structural layout optimization of tall buildings subjected to dynamic wind loads. J Struct Eng. https://doi.org/10.1061/JSENDH.STENG-12366

Aschheim M, Hernández-Montes E, Gil-Martín L (2007) Optimal domains for strength design of rectangular sections for axial load and moment according to Eurocode 2. Eng Struct 29(8):1752–1760

Aschheim M, Hernández-Montes E, Gil-Martín L (2018) Design of optimally reinforced RC beam, column and wall section. J Struct Eng 134(2):169–188

Aydın Y, Bekdaş G, Nigdell SM, Isikdag U, Kim S, Geem ZW (2023) Machine learning models for ecofriendly optimum design of reinforced concrete columns. Appl Sci 13(7):4117

Babu JS, Mahendran N (2013) Design criteria for reinforced concrete columns under seismic loading. Int J Eng. https://doi.org/10.17577/IJERTV2IS4363

Barros MHFM, Barros AFM, Ferreira CA (2004) Closed form solution of optimal design of rectangular reinforced concrete sections. Eng Struct 21(7):761–776

Bock T (2015) The future of construction automation: technological disruption and the upcoming ubiquity of robotics. Autom Constr 59:113–121

Building and Construction Authority (BCA) (2004) Code of practice on buildable design. BCA

Carbonell-Márquez JF, Gil-Martin LM, Fernández-Ruiz MA. Hernández-Montes E (2014) Asymmetrically reinforced concrete piles in earth retaining systems. In: 37th IABSE international symposium, Madrid, 2014, vol 102, pp 468–469

Chai SYW, Ngu LH, How BS, Chin MY, Abdouka K, Adini MJBA, Kassim AM (2022) Review of CO_2 capture in construction-related industry and their utilization. Int J Greenh Gas Control 119:103727

Chatterjee S, Sarkar S, Hore S, Dey N, Ashour AS, Shi F, Le D-N (2007) Structural failure classification for reinforced concrete buildings using trained neural network based multi-objective genetic algorithm. Struct Eng Mech 63(4):429–438

Chen Y, Oudan GE, Riley DR (2010) Decision support for construction method selection in concrete buildings: prefabrication adoption and optimization. Autom Constr 19(6):665–675

Chen JH, Yan S, Tai H-W, Chang C-Y (2017) Optimizing profit and logistics for precast concrete production. Can J Civ Eng. https://doi.org/10.1139/cjce-2016-0401

Chou J-S, Liu C-Y, Prayogo H, Khasani RR, Gho D, Lalitan GG (2022) Predicting nominal shear capacity of reinforced concrete wall in building by metaheuristics-optimized machine learning. J Build Eng 61:105046

Coello CC, Christiansen AD, Hernández SF (1997) GA simple genetic algorithm for the designs of reinforced concrete beams. Eng Comput. https://doi.org/10.1007/BF01200046

Coello CAC, Lamont GB, Van Veldhuizen DA (2007) Evolutionary algorithms for solving multi-objective problems. Springer, New York

Deb K, Pratap A, Agarwal S, Meyarivan T (2002) A fast and elitist multiobjective genetic algorithm: NSGA-II. IEEE Trans Evol Comput 6(2):124–141

Devenes J, Bastien-Masse M, Fivet C (2024) Reusability assessment of reinforced concrete components prior to deconstruction from obsolete buildings. J Build Eng 84(1):108584

Eleftheriadis S, Duffour P, Stephenson B, Mumovic D (2018) Automated specification of steel reinforcement to support the optimisation of RC floors. Autom Constr 96:366–377

European Union (2004) EN1992-1-1, Eurocode 2: design of concrete structures—Part 1-1: general rules and rules for buildings. EU, Maastricht

Fernández-Ceniceros J, Fernandez-Martinez R, Fraile-Garcia E, Martinez-de-Pison FJ (2013) Decision support model for one-way floor slab design: a sustainable approach. Autom Constr 35:460–470

Fischer M, Tatum CB (1997) Characteristics of design-relevant constructability knowledge. J Eng Manag 123(3):253–260

Gandomi AH, Kashani AR, Roke DA, Mousavi M (2015) Optimization of retaining wall design using recent swarm intelligence techniques. Eng Struct 103:72–84

García de Soto B, Agustí-Juan I, Hunhevicz J, Joss S, Graser K, Habert G, Adey BT (2018) Productivity of digital fabrication in construction: cost and time analysis of a robotically built wall. Autom Constr 92:297–311

Gil-Martín LM, Hernández-Montes E, Aschheim M (2010) Optimal reinforcement of RC columns for biaxial bending. Mater Struct J 43:1245–1256

Gil-Martín LM, Aschheim M, Hernandez-Montes E, Pasadas-Fernandez M (2011) Recent developments in optimal reinforcement of RC beam and column sections. Eng Struct 33:1170–1180

Hernández-Montes E, Aschheim M, Gil-Martin LM (2004) Impact of optimal longitudinal reinforcement on the curvature ductility capacity of reinforced concrete column section. Mag Concr Res 56(9):499–512

Jahjouh MM, Arafa M, Alqedra MA (2013) Artificial bee colony (ABC) algorithm in the design optimization of RC continuous beams. Struct Multidisc Optim 47:63–79

Koumousis VK, Arsenis SJ (1998) Genetic algorithms in optimal detailed design of reinforced concrete members. Comput Aided Civ Infrastruct Eng 13(1):43–52

Lao W-L, Li M, Wong BCL, Gan VJL, Cheng JCP (2023) BIM-based constructability-aware precast building optimization using optimality criteria and combined non-dominated sorting genetic II and great deluge algorithm (NSGA-II-GD). Autom Constr 155:169–188

Latif I, Banerjee A, Surana M (2022) Explainable machine learning aided optimization of masonry infilled reinforced concrete frames. Structures 44:1751–1766

Lee HJ, Aschheim M, Hernandez-Montes E, Gil-Martin LM (2009) Optimum RC column reinforcement considering multiple load combinations. Struct Multidisc Optim 39:153–170

Lepš M, Sejnoha M (2003) New approach to optimization of reinforced concrete beams. Comput Struct 81:1957–1966

Li M, Wong BCL, Liu Y, Chan CM, Gan VJL, Cheng JCP (2021) DfMA-oriented design optimization for steel reinforcement using BIM and hybrid meta-heuristic algorithms. J Build Eng 44:103310

Li M, Liu Y, Wong BCL, Gan VJL, Cheng JCP (2023) Automated structural design optimization of steel reinforcement using graph neural network and exploratory genetic algorithms. Autom Constr 146:104677

Liu J, Liu P, Feng L, Wu W, Li D, Chen YF (2020) Automated clash resolution for reinforcement steel design in concrete frames via Q-learning and building information modeling. Autom Constr 112:103062

Lou H, Gao B, Jin F, Wan Y, Wang Y (2021) Shear wall layout optimization strategy for high-rise buildings based on conceptual design and data-driven Tabu search. Comput Struct 250:106546

L'udovit F, Marek C, Porubsky T (2013) Reliability of asymmetrically reinforced columns. Concr Concr Struct 65:387–392

Mahmoudian A, Tajik N, Taleshi MM, Shakiba M, Yekrangnia M (2023) Ensemble machine learning-based approach with genetic algorithm optimization for predicting bond strength and failure mode in concrete-GFRP mat anchorage interface. Structures 57:105173

Mangal M, Cheng JCP (2018) Automated optimization of steel reinforcement in RC building frames using building information modeling and hybrid genetic algorithm. Autom Constr 90:39–57

Mangal M, Li M, Gan VJL, Cheng JCP (2021) Automated clash-free optimization of steel reinforcement in RC frame structures using building information modeling and two-stage genetic algorithm. Autom Constr 126:103676

McCormac JC, Brown RH (2013) Design of reinforced concrete, 9th edn. Wiley, Hoboken

Moussavi Nadoushani ZS, Akbarnezhad A (2015) Effects of structural system on the life cycle carbon footprint of buildings. Energy Build 102:337–346

Nigdeli SM, Yücel M, Bekdas G (2023) A hybrid artificial intelligence model for design of reinforced concrete columns. Neural Comput Appl 35:7867–7875

Park HS, Lee H, Kim Y, Hong T, Choi SW (2014) Evaluation of the influence of design factors on the CO_2 emissions and costs of reinforced concrete columns. Energy Build 82:378–384

Pasandideh SHR, Niaki STA, Asadi K (2015) Bi-objective optimization of a multi-product multi-period three-echelon supply chain problem under uncertain environments: NSGA-II and NRGA. Inf Sci 292:57–74

Pierott R, Hammad AWA, Haddad A, Garcia S, Falcon G (2021) A mathematical optimisation model for the design and detailing of reinforced concrete beams. Eng Struct 245:112861

Rafiq MY, Southcombe C (1998) Genetic algorithms in optimal design and detailing of reinforced concrete biaxial columns supported by a declarative approach for capacity checking. Comput Struct 69(4):443–457

Raue E, Hahn S (2005) Optimum reinforcement design of concrete cross-sections considering deformation constraints. J Civ Eng Manag 11(1):65–71

Sánchez-Olivares G, Tamas A (2017) Improvements in meta-heuristic algorithms for minimum cost design of reinforced concrete rectangular sections under compression and biaxial bending. Eng Struct 130:162–179

Tanhadoust A, Madhkhan M, Nehdi ML (2023) Two-stage multi-objective optimization of reinforced concrete buildings based on non-dominated sorting genetic algorithm (NSGA-III). J Build Eng 75:107022

Verduzco LF, Horta J, Hernandez MAPL, Hernandez JB (2022) CALRECOD—a software for Computed Aided Learning of REinforced COncrete structural Design. Adv Eng Softw 172:103189

Wahde M (2008) Biologically inspired optimization methods. An introduction. WIT Press, Southampton

Xu C, Liu J, Wu Z, Chen YF (2022) Automated steel reinforcement detailing in reinforced concrete frames using evolutionary optimization and artificial potential field. Autom Constr 138:104224

Yeh JP, Chen KY (2012) Forecasting the lowest cost and steel ratio of reinforced concrete simple beams using the neural network. J Civ Eng Constr Technol 3(3):99–107

Yeo D, Gabbai RD (2011) Sustainable design of reinforced concrete structures through embodied energy optimization. Energy Build 43(8):2028–2033

Yuan Z, Sun C, Wang Y (2018) Design for manufacture and assembly-oriented parametric design of prefabricated buildings. Autom Constr 88:13–22

Zhao P, Liao W, Huang Y, Lu X (2024) Beam layout design of shear wall structures based on graph neural networks. Autom Constr 158:105223

Publisher's Note Springer Nature remains neutral with regard to jurisdictional claims in published maps and institutional affiliations.